

# Measurements of carbonyl compounds around the Arabian Peninsula: overview and model comparison

Nijing Wang<sup>1</sup>, Achim Edtbauer<sup>1</sup>, Christof Stönnner<sup>1</sup>, Andrea Pozzer<sup>1</sup>, Efstratios Bourtsoukidis<sup>1</sup>, Lisa Ernle<sup>1</sup>, Dirk Dienhart<sup>1</sup>, Bettina Hottmann<sup>1</sup>, Horst Fischer<sup>1</sup>, Jan Schuladen<sup>1</sup>, John N. Crowley<sup>1</sup>, Jean-Daniel Paris<sup>2</sup>, Jos Lelieveld<sup>1,3</sup>, Jonathan Williams<sup>1,3</sup>

<sup>1</sup>Air Chemistry Department, Max Planck Institute for Chemistry, Hahn-Meitner-Weg 1, 55128 Mainz, Germany

<sup>2</sup>Laboratoire des Sciences du Climat et de l'Environnement, LSCE/IPSL, CEA-CNRS-UVSQ, Université Paris-Saclay, Gif-sur-Yvette, France

<sup>3</sup>Energy, Environment and Water Research Center, The Cyprus Institute, Nicosia, Cyprus

*Correspondence to:* Nijing Wang (nijing.wang@mpic.de)

## Abstract

Volatile organic compounds (VOCs) were measured around the Arabian Peninsula using a research vessel during the AQABA campaign (Air Quality and Climate Change in the Arabian Basin) from June to August 2017. In this study we examine carbonyl compounds, measured by a proton transfer reaction mass spectrometer (PTR-ToF-MS), and present both a regional concentration distribution and a budget assessment for these key atmospheric species. Among the aliphatic carbonyls, acetone had the highest mixing ratios in most of the regions traversed, varying from 0.43 ppb over the Arabian Sea to 4.5 ppb over the Arabian Gulf, followed by formaldehyde (measured by Hantzsch monitor, 0.82 ppb over the Arabian Sea and 3.8 ppb over the Arabian Gulf) and acetaldehyde (0.16 ppb over the Arabian Sea and 1.7 ppb over the Arabian Gulf). Unsaturated carbonyls (C4-C9) varied from 10 to 700 ppt during the campaign, and followed similar regional mixing ratio dependence as aliphatic carbonyls, which were identified as oxidation products of cycloalkanes over polluted areas. We compared the measurements of acetaldehyde, acetone and methyl ethyl ketone to global chemistry-transport model (EMAC) results. A significant discrepancy was found for acetaldehyde, with the model underestimating the measured acetaldehyde mixing ratio by up to an order of magnitude. Implementing a photolytically driven marine source of acetaldehyde significantly improved the agreement between measurements and model, particularly over the remote regions (e.g. Arabian Sea). However, the newly introduced acetaldehyde source was still insufficient to describe the observations over the most polluted regions (Arabian Gulf and Suez), where model underestimation of primary emissions and biomass burning events are possible reasons.

## 36 1 Introduction

37 Carbonyl compounds (aldehydes and ketones) can be released into the air directly from a variety of primary biogenic and  
38 anthropogenic sources. These include biomass burning (Holzinger et al., 1999; Holzinger et al., 2005; Koss et al., 2018), fossil fuel  
39 combustion (Reda et al., 2014; Huang et al., 2018) including vehicles (Erickson et al., 2014; Dong et al., 2014), industrial solvent  
40 use (Kim et al., 2008), and natural sources including plants and plankton (Zhou and Mopper, 1997; Warneke et al., 1999; Jacob et  
41 al., 2002; Fall, 2003; Williams et al., 2004; Bourtsoukidis et al., 2014). However, secondary production via the atmospheric  
42 oxidation of hydrocarbons is considered to be more important for many carbonyl compounds including acetone and acetaldehyde  
43 (Jacob et al., 2002; Millet et al., 2010).

44 Carbonyls have several important roles in the atmosphere. They form as stable intermediates directly after hydrocarbon oxidation  
45 by hydroxyl radicals,  $O_3$  or  $NO_3$ , when the peroxy radicals initially formed react with each other (permutation reactions) or with  
46  $NO$ . Their production is linked to tropospheric ozone formation (Carlier et al., 1986) and their loss, through oxidation and  
47 photolysis, is an important source of hydroxyl and hydroperoxyl radicals ( $HO_x$ ) in the dry upper troposphere (Colomb et al., 2006).  
48 Carbonyls serve as precursors of peroxyacetyl nitrates (PANs) which are important atmospheric  $NO_x$  ( $NO$  and  $NO_2$ ) reservoir  
49 species (Finlayson-Pitts and Pitts, 1997; Edwards et al., 2014; Williams et al., 2000). Carbonyl compounds are also important for  
50 the growth of atmospheric particles (Kroll et al. 2005) thereby indirectly impacting the Earth's radiative balance. The atmospheric  
51 lifetimes of carbonyl compounds varies considerably, from less than one day for acetaldehyde (Millet et al., 2010) to more than 15  
52 days for acetone (Jacob et al., 2002; Khan et al., 2015) in terms of tropospheric mean lifetime. A multiday lifetime means that  
53 carbonyl compounds can impact the air chemistry on local, regional and even hemispheric scales. The numerous primary and  
54 secondary sources of carbonyl compounds, as well as their multiple loss routes (photolysis,  $OH$ ,  $NO_3$  and  $O_3$  oxidation) makes  
55 budget assessments difficult.

56 The most predominant atmospheric carbonyl compounds besides formaldehyde are acetaldehyde and acetone. They have been  
57 reported to vary from tens or hundreds of ppt in remote areas (Warneke and de Gouw, 2001; Wisthaler, 2002; Lewis et al.,  
58 2005; White et al., 2008; Colomb et al., 2009; Read et al., 2012; Sjostedt et al., 2012; Tanimoto et al., 2014; Yang et al.,  
59 2014; Hornbrook et al., 2016; Wang et al., 2019) to several ppb in urban and polluted areas (Dolgorouky et al., 2012; Guo et al.,  
60 2013; Stoeckenius and McNally, 2014; Koss et al., 2015; Sahu et al., 2017; Sheng et al., 2018). Generally, secondary photochemical  
61 formation from various precursors is the main source for those carbonyl compounds. However, several recent studies have shown  
62 that acetaldehyde mixing ratios in both the remote marine boundary layer and the free troposphere could not be explained by  
63 known photochemistry as implemented in various atmospheric chemistry models, which consistently underestimated the  
64 measurements by an order of magnitude or more (Singh et al., 2003; Read et al., 2012; Wang et al., 2019). Several potential  
65 additional acetaldehyde sources have been proposed including new hydrocarbon oxidation mechanisms, aerosol related sources  
66 and oceanic sources. One possible source of acetaldehyde in the remote marine boundary layer is oceanic emission from the photo  
67 degradation of colored dissolved organic matter (CDOM) in sea-surface water, where acetaldehyde could be produced together  
68 with other low molecular weight carbonyl compounds (Kieber et al., 1990; Zhou and Mopper, 1997; Sinha et al., 2007; Dixon et al.,  
69 2013). Nevertheless, due to both limited airborne and seawater measurements of acetaldehyde, the importance of oceanic emission  
70 is still under debate (Millet et al., 2010; Wang et al., 2019). In order to better understand the atmospheric budgets of acetaldehyde  
71 (and the other carbonyl compounds), it is informative to analyze a dataset of multiple carbonyl compounds in both polluted and  
72 clean environments, with influence from marine emissions, varying particulate loadings, and high rates of oxidation as shown in  
73 Figure 1, which demonstrates the main formation pathways of acetaldehyde during this campaign.

During the shipborne research campaign AQABA, carbonyl compounds were continuously measured by PTR-ToF-MS onboard a research vessel that circumnavigated the Arabian Peninsula. During the campaign, chemically distinct air masses were sampled, which had been influenced by primary emissions of hydrocarbons and inorganic pollutants ( $\text{NO}_x$ ,  $\text{SO}_2$  and  $\text{CO}$ ) from petroleum industries and marine transport (Bourtsoukidis et al., 2019; Celik et al., 2019), by pollution from urban areas (Pfannerstill et al., 2019), and clean marine influenced air (Edtbauer et al., 2020). It is a unique dataset of carbonyl compounds encompassing starkly different environmental conditions from a region with few (or none) available in-situ measurements to date.

In this study, we provide an overview of carbonyl compound mixing ratios (aliphatic, unsaturated and aromatic) over the Mediterranean Sea, Suez, Red Sea, Arabian Sea and Arabian Gulf. Using an empirical method based on measured hydrocarbon precursors, we have analyzed the relative importance of the photochemical sources for the carbonyl compounds observed. The analysis is then extended to include sources and transport by using a global model EMAC (5th generation European Centre – Hamburg general model, ECHAM5 coupled to the modular earth submodel system, MESSy, applied to atmospheric chemistry). Model measurement differences are investigated in both clean and polluted regions, with particular emphasis on acetaldehyde.

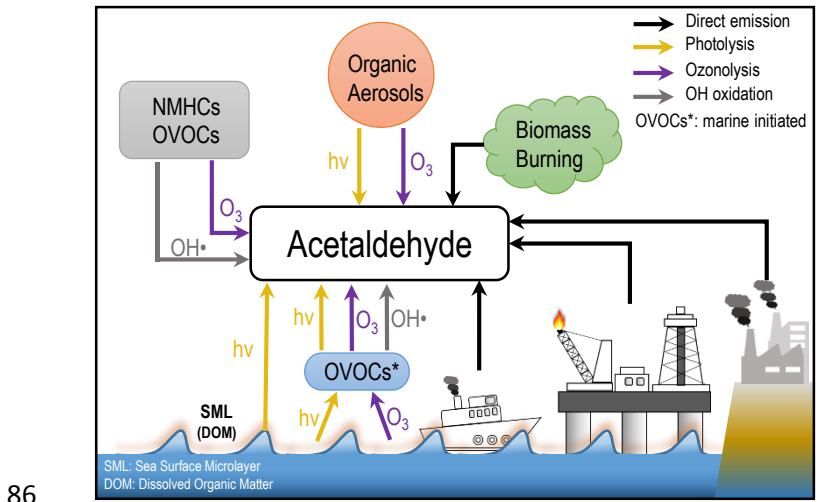


Figure 1. Diagram of possible sources and formation pathways of acetaldehyde during the AQABA campaign.

## 2 Methods

### 2.1 AQABA campaign

The AQABA campaign was conducted onboard the research vessel Kommandor Iona (KI) from the end of June to the end of August 2017. The ship started from Southern France, proceeded across the Mediterranean, through the Suez Canal, around the Arabian Peninsula into the Arabian Gulf and on to Kuwait, thereafter returning along the same route. Five laboratory containers were loaded onto the vessel, containing multiple gas and particle phase measurement instruments as well as a weather station.

### 2.2 PTR-ToF-MS

#### 2.2.1 Sampling and instrument set-up

A high-flow inlet (stainless steel tubing, 0.2 m diameter, 5.5 m tall and 3 m above the top of the containers and the front deck) was installed at the front of the ship where the laboratory containers were located. A high flow of air (approximately  $10 \text{ m}^3 \text{ min}^{-1}$ ) was drawn through the inlet which provided a common attachment point for sub-sampling lines for all gas-phase measurement instruments. An air flow of  $5 \text{ standard L min}^{-1}$  for the first leg and  $3.5 \text{ standard L min}^{-1}$  for the second leg was pumped into the

on-board lab container through an 1/2" (O.D. = 1.27cm) FEP (fluorinated ethylene propylene) tubing (about 10 m long) insulated and heated to 50-60 °C. A PTFE (polytetrafluoroethylene) filter was placed at the beginning of the inlet to prevent insects, dust and particles entering the instruments. Every 2-5 days, the filter was replaced depending on the degree of pollution encountered. Inside the VOC instrument container, the PTR-ToF-MS (8000, Ionicon Analytik GmbH Innsbruck, Austria) sampled a sub-flow at 80-100 sccm through 1/8" (0.3175 cm) FEP tubing (~ 10 m in length, insulated and heated to 60 °C) from the main fast air flow and then to the instrument's PEEK (polyether ether ketone) inlet which was likewise heated to 60 °C. The inlet system was shared with total OH reactivity measurement (Pfannerstill et al., 2019).

The working principle of PTR-MS has been described in detail in previous studies (Lindinger et al., 1998; Ellis and Mayhew, 2013; Yuan et al., 2017). In brief,  $\text{H}_3\text{O}^+$  primary ions are generated in the ion source, and then drawn into the drift tube where they interact with sampled ambient air. Inside the drift tube, VOCs with a proton affinity greater than that of  $\text{H}_2\text{O}$  (691 kJ mol<sup>-1</sup>) are protonated by proton transfer from  $\text{H}_3\text{O}^+$ . The resulting secondary ions are transferred to the detector, in this case a time-of-flight mass spectrometer with mass resolution around 3500 for the first leg and 4500 for the second leg at mass 96amu. An internal standard of trichlorobenzene ( $\text{C}_6\text{H}_3\text{Cl}_3$ ) was continuously introduced into the instrument to ensure accurate mass calibration. Every minute a spectrum with mass range (m/z) 0-450 was generated. The data reported in this study are all at 1 minute resolution unless otherwise specified.

## 2.2.2 Instrument characterization

The instrument background was determined every three hours for 10 minutes with synthetic air. 4-point calibrations were performed five times during the whole campaign using a standard gas mixture (Apel-Riemer Environmental inc., Broomfield, USA) containing 14 compounds (methanol, acetonitrile, acetaldehyde, acetone, dimethyl sulfide, isoprene, methyl vinyl ketone, methacrolein, methyl ethyl ketone, benzene, toluene, xylene, 1,3,5-trimethylbenzene and  $\alpha$ -pinene). It has been previously reported that the sensitivity of some compounds measured by PTR-MS are humidity dependent (de Gouw and Warneke, 2007). As the relative humidity (RH) was expected to be high and varying (marine boundary layer with occasional desert air influence), humidity calibration was combined with 4-point calibration by humidifying the gas mixture at different levels from 0% - 100% RH.

## 2.2.3 Data analysis

The data were initially processed by the PTR Analyzer software (Müller et al., 2013) to identify and integrate the peaks. After obtaining the raw data (counts per second for each mass identified), a custom-developed python-based program was used to further process the data to final mixing ratios. For compounds present in the standard gas cylinder, interpolated sensitivities based on the five in-campaign calibrations were applied to derive the mixing ratios; while mixing ratios of the other masses were calculated by using a proton transfer reaction rate constant ( $k_{PTR}$ ) of  $2.0 \times 10^{-9} \text{ cm}^3 \text{ s}^{-1}$ . The uncertainty associated with the mixing ratios of the calibrated compounds was around 6-17% (see Table S1). For the mixing ratios derived by assuming  $k_{PTR}$ , the accuracy was around  $\pm 50\%$  (Zhao and Zhang, 2004). The detection limit (LOD) was calculated from the background measurement with 3 times the standard deviation ( $3\sigma$ ),  $52 \pm 26$  ppt for acetaldehyde,  $22 \pm 9$  ppt for acetone and  $9 \pm 6$  ppt for methyl ethyl ketone (MEK) (Table S1). Data below LOD were excluded from the data set instead of giving zero.

In this study, we have interpreted ion masses with the exact masses corresponding to  $\text{C}_n\text{H}_{2n}\text{O}$ ,  $\text{C}_n\text{H}_{2n-2}\text{O}$  and  $\text{C}_n\text{H}_{2n-8}\text{O}$  as aliphatic, unsaturated and aromatic carbonyls, respectively (see exact protonated m/z in Table S2). Carbonyl compounds with a carbon number of three and above can be either aldehydes or ketones, which are not distinguishable with PTR-ToF-MS using  $\text{H}_3\text{O}^+$  as the primary ion. However, laboratory experiments have shown that protonated aldehydic ions with carbon atoms more than three tend

138 to lose a H<sub>2</sub>O molecule and fragment to other masses (Buhr et al., 2002;Spanel et al., 2002). Moreover, although both ketones and  
139 aldehydes can be produced via atmospheric oxidation processes, ketones tend to have longer atmospheric lifetimes and higher  
140 photochemical yields than aldehydes as mentioned in the introduction. The ratio of measured propanal to acetone was 0.07 in the  
141 western Pacific costal region (Schlundt et al., 2017), 0.06 in an urban Los Angeles (Borbon et al., 2013) and 0.17 - 0.22 in oil & gas  
142 production regions (summarized by Koss et al., 2017). Therefore, signals on the exact mass of carbonyl compounds from the PTR-  
143 ToF-MS are expected to be dominated by ketones, particularly in regions remote from the sources.

### 144 2.3 Meteorological data and other trace gases

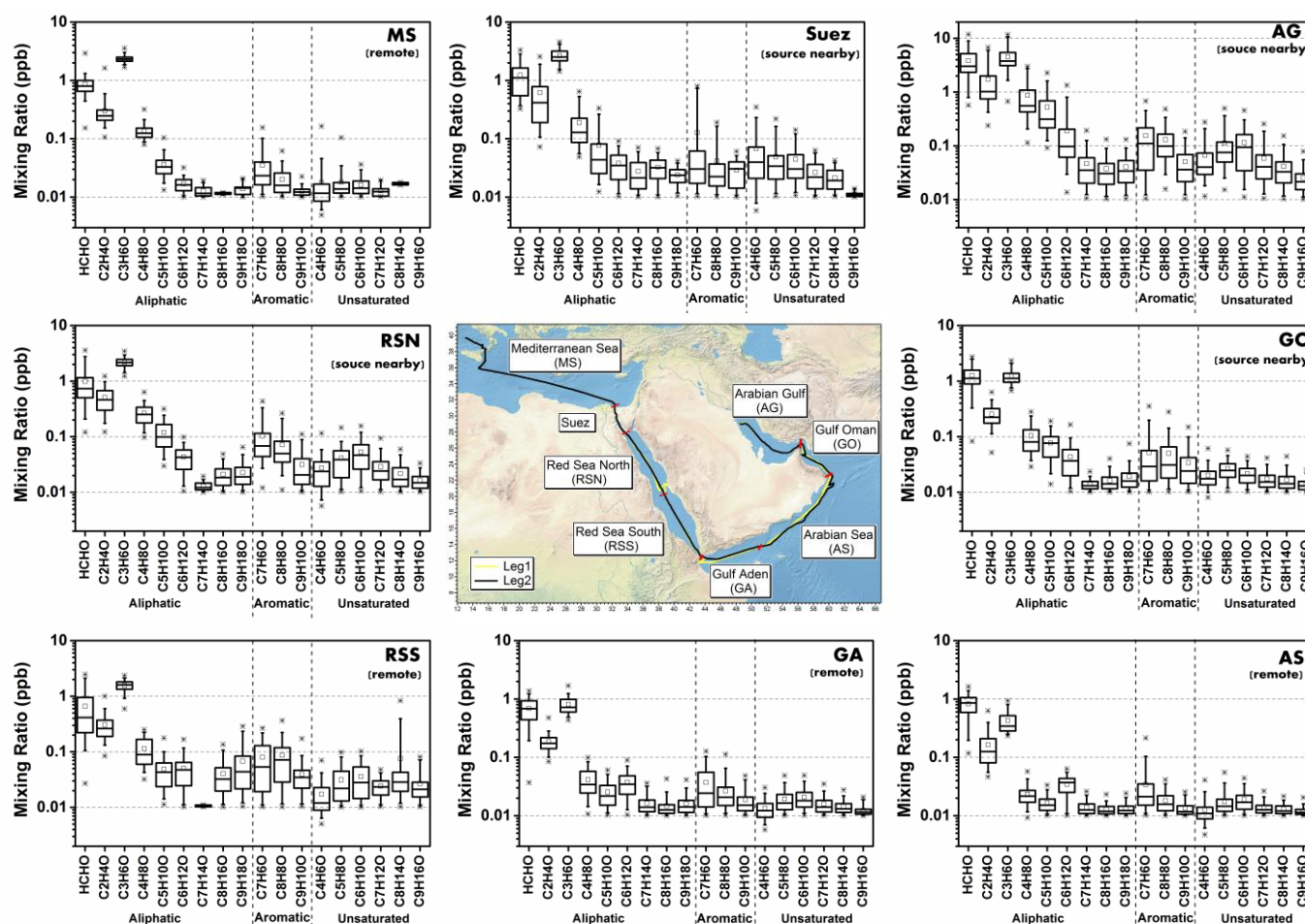
145 The meteorological data were obtained by using a commercial weather-station (Sterela) which monitored wind speed, wind  
146 direction, relative humidity (RH), temperature, speed of the vessel, and GPS etc. The actinic flux was measured by a spectral  
147 radiometer (Metcon GmbH; Meusel et al., 2016). Non methane hydrocarbons (NMHC) mixing ratios were measured by a gas  
148 chromatograph with flame ionization detector (GC-FID) online with the time resolution of 50 minutes. It measured hydrocarbons  
149 (C<sub>2</sub>-C<sub>8</sub>) and aromatics (C<sub>6</sub>-C<sub>8</sub>) with the average LOD < 10 ppt for most of compounds. For a detailed instrumental description  
150 see Bourtsoukidis et al. (2019). Formaldehyde mixing ratios were determined by a modified and optimized version of the  
151 commercially available AL4021 (Aero-Laser, Germany), which utilizes the Hantzsch technique (Stickler et al., 2006). Methane  
152 and carbon monoxide (CO) levels were monitored by a cavity ring-down spectroscopy analyzer (Picarro G2401). Ozone was  
153 measured with an absorption photometer (Model 202 Ozone Monitor, 2B Technologies, Boulder, Colorado). Due to the potential  
154 interference from sampling our own ship exhaust in which carbonyl compounds may be present (Reda et al., 2014), a filter was  
155 applied to the data set based on the wind direction and NO<sub>x</sub>, SO<sub>2</sub> and ethene levels.

### 156 2.4 Model simulations

157 The EMAC (ECHAM5/MESSy Atmospheric Chemistry) model was used to simulate atmospheric mixing ratios of several  
158 carbonyl compounds along the cruise track covered during the AQABA campaign. The EMAC model is an atmospheric chemistry-  
159 general circulation model simulating the process of tropospheric air by considering processes which could influence trace gases  
160 mixing ratios, such as transport, chemistry, interaction with ocean/land, dry deposition and so on (Pozzer et al., 2007;Pozzer et al.,  
161 2012;Lelieveld et al., 2016). The model applied in this study is a combination of the 5<sup>th</sup> generation of European Centre Hamburg  
162 general circulation model (ECHAM5) (Roeckner et al., 2006) and the 2<sup>nd</sup> version of Modular Earth Submodel System (MESSy2)  
163 (Jöckel et al., 2010), where a comprehensive chemistry mechanism MOM (Mainz Organic Mechanism) was deployed (Sander et  
164 al., 2019). The model considers direct emissions (such as anthropogenic, biogenic, biomass burning etc.), atmospheric transport  
165 and mixing, photochemical production of carbonyls (by OH, O<sub>3</sub> and NO<sub>3</sub>), as well as physical and chemical removal processes.  
166 The global fire assimilation system was used for biomass burning emissions (Kaiser et.al., 2012). The exchange of organic  
167 compounds between ocean and atmosphere was considered in EMAC via the AIRSEA submodel, described in detail in Pozzer et  
168 al. (2006). The transfer velocity is calculated online and the concentration in the water is prescribed by the user. For acetone, a  
169 constant water concentration of 15 nmol/L is used, following the suggestion of Fischer et al. (2012). The model configuration in  
170 the study is the same as the model applied in Bourtsoukidis et al. (2020), where a natural non-methane hydrocarbon source (ethane  
171 and propane) was implemented. The model is in the resolution of T106L31 (i.e. ~ 1.1° × 1.1° horizontal resolution and , 31 vertical  
172 hybrid pressure levels up to 10 hPa) and the time resolution of 10 minutes. The measurement data of PTR-ToF-MS were averaged  
173 to 10-minute resolution to match the model data resolution for further comparison.

174

176 Around the Arabian Peninsula, the mixing ratios of individual carbonyl compounds varied over a wide range, from tens of ppt to  
 177 ppb levels. In this study, we divided the dataset geographically into eight regions (Figure 2, middle graph) to classify and  
 178 characterize the primary and secondary origins of carbonyl compounds. The regional delineations were: the Mediterranean Sea  
 179 (MS), Suez, Red Sea North (RSN), Red Sea South (RSS), Gulf of Aden (GA), Arabian Sea (AS), Gulf of Oman (GO) and Arabian  
 180 Gulf (AG), the same as those described by Bourtsoukidis et al. (2019). Figure 2 shows the abundance of aliphatic, aromatic and  
 181 unsaturated carbonyl compounds (carbonyls) for each region. Generally, aliphatic carbonyls were present at much higher mixing  
 182 ratios than aromatic and unsaturated carbonyls, with smaller carbonyl compounds (formaldehyde, acetaldehyde, C3 and C4  
 183 carbonyls) dominating the distribution. The mixing ratios of aliphatic carbonyls decreased dramatically from C5 carbonyls with  
 184 increasing carbon number. The box plots (Figure 2) also show that carbonyl compounds were measured at higher mixing ratios  
 185 and were more variable over Suez region and the Arabian Gulf. The abundance of carbonyl compounds varied markedly from  
 186 region to region with highest and lowest values found in the Arabian Gulf and the Arabian Sea, respectively. Table 1 shows the  
 187 mean, standard deviation and the median values for carbonyls in each region. In the following sections, each class of carbonyl  
 188 compounds are investigated in greater detail.



189 Figure 2. Overview of mixing ratios for aliphatic, aromatic and unsaturated carbonyl compounds ( $C_xH_yO$ ). The boxes represent  
 190 25% to 75% of the data with the central line and square indicating the median and the mean values, respectively. The whiskers  
 191 show data from 5% to 95% and stars were drawn for the minimum and maximum data points within 1% to 99% of the dataset.  
 192 Within brackets under the region acronyms the main characteristics of the air masses are indicated, based on non-methane  
 193 hydrocarbon variability-lifetime results (b factor) from Bourtsoukidis et al. (2019). The data used for map plotting was from public  
 194

domain GIS data found on the Natural Earth web site (<http://www.naturalearthdata.com>) and was read into Igor using the IgorGIS XOP beta.

### 3.1 Aliphatic carbonyls (C<sub>n</sub>H<sub>2n</sub>O)

#### 3.1.1 Overview

Relatively high mean mixing ratios of aliphatic carbonyls were observed over the Arabian Gulf; the highest being acetone (C3 carbonyl compound) at  $4.50 \pm 2.40$  ppb (median: 3.77 ppb), followed by formaldehyde at  $3.83 \pm 2.55$  ppb (median: 3.02 ppb), acetaldehyde at  $1.73 \pm 1.61$  ppb (median: 1.02 ppb) and MEK (C4 carbonyl compound) at  $0.87 \pm 0.71$  ppb (median: 0.56 ppb). As the Arabian Gulf is highly impacted by the oil and gas industry, we compared the measurements of the four aforementioned carbonyl compounds with those measured in the oil and gas region (Table 2). Expect for formaldehyde, acetaldehyde, acetone and MEK were lower than the mixing ratios measured in the Uintah Basin, which was influenced by intensive oil and natural gas activities (Koss et al., 2015). The general distribution of the aliphatic carbonyls in the Uintah Basin is similar to the Arabian Gulf, with acetone levels being approximately twice as those of acetaldehyde. The carbonyl mixing ratios in the Arabian Gulf were comparable to those measured in Hickory (PA, USA) surrounded by natural gas wells (Swarthout et al., 2015). Koss et al. (2017) reported the max boundary layer enhancement of carbonyl compounds (C2-C7) measured during an aircraft measurement above the most productive oil field in the United States (Permian Basin). Within the boundary layer of the Permian Basin, C5-C7 aliphatic carbonyls had mixing ratios of 0.34 ppb, 0.08 ppb and 0.03 ppb; which are of the same magnitude but lower than the levels measured over the Arabian Gulf for C5 ( $0.52 \pm 0.48$  ppb), C6 ( $0.19 \pm 0.25$ ppb) and C7 ( $0.05 \pm 0.04$  ppb) carbonyl compounds. The sources of the major carbonyls in the Arabian Gulf will be discussed in details in section 3.1.2 and 3.4.3.

In contrast, aliphatic carbonyls had much lower average mixing ratios over the Arabian Sea and the Gulf of Aden especially for C7-C9 carbonyls with mean mixing ratios below the detection limit for most of the time. During the summertime AQABA campaign, the prevailing wind direction over the Arabian Sea was southwest (Figure S1). Four-day back trajectories indicate the air was transported from the Arabian Sea (Northwestern Indian Ocean), passing East Africa coast, which brought relatively clean, photochemically aged airmasses (Bourtsoukidis et al., 2019). The mean level of acetone over the Arabian Sea ( $0.43 \pm 0.18$  ppb, median: 0.34 ppb) is close to the level measured in the marine boundary layer of Western Indian Ocean (0.49 ppb) (Warneke and de Gouw, 2001) and comparable to other reported values from open-sea air measurement (see Table 2). Acetaldehyde was measured at relatively low mixing ratios over the Arabian Sea ( $0.16 \pm 0.12$  ppb, median: 0.13 ppb), which is comparable than the levels reported by the measurements done in northern-hemisphere open ocean (see, Table 2). Over the Gulf of Aden, acetone and MEK had slightly higher mixing ratios than those over the Arabian Sea.

The Mediterranean Sea had somewhat higher levels of aliphatic carbonyls than the clean regions (the Arabian Sea and the Gulf of Aden) but with acetone (above 2ppb) dominating the distribution. Much higher acetone level than acetaldehyde level was also observed for some costal site measurement which was impacted by continental air (White et al., 2008; Schlundt et al., 2017, see Table 2). Larger aliphatic carbonyls (C6-C9) were below the detection limit most of the time. The aliphatic carbonyls levels over the Gulf of Oman were higher than the clean regions, while C1-C5 carbonyls were more variable over the Gulf of Oman compared to those over the Mediterranean Sea. This is probably because the Gulf of Oman connects to the Arabian Gulf where intense oil and gas industrial activities are located. Over the Gulf of Oman, polluted air from the nearby sources of the Arabian Gulf is occasionally mixed with the clean air from the open sea (the Arabian Sea) under southeast wind conditions (Figure S1).

Another region where abundant aliphatic carbonyls were observed was Suez region. The air in this region was mainly influenced by nearby cities and marine transportation (ship emissions within the Suez Chanel) (Bourtsoukidis et al., 2019; Pfannerstill et al.,

2019). Therefore abundant precursors were available in Suez region, producing more carbonyls regionally especially for shorter-lived compounds (formaldehyde and acetaldehyde). Besides the local-scale emissions and photochemical production contribution to the carbonyls over Suez, the longer lived carbonyls (e.g. acetone) could be also transported from the Mediterranean Sea (where acetone was high). Four-day back trajectories indicate the air reaching Suez region was mostly originated from Europe continent passing over the Mediterranean Sea (Bourtsoukidis et al., 2019). Meanwhile, ocean uptake of acetone from the air due to polluted continental outflow (Marandino et al., 2005) as well as dilution and mixing with free tropospheric air during transport can modulate acetone mixing ratios. Although the mean mixing ratios of aliphatic carbonyls over Suez were much lower than those over the Arabian Gulf, the variations were still more significant than other regions (not including the Arabian Gulf, see Table 1).

Over the Red Sea, acetone was the most abundant aliphatic carbonyls followed by formaldehyde and acetaldehyde. The mixing ratios of acetaldehyde and acetone over the northern part of the Red Sea were similar to those levels measured in western Pacific coastal regions (South China Sea, Table 2). It is worth noticing that the levels of aliphatic carbonyls in the northern part of the Red Sea were almost two times higher than the southern part of the Red Sea. According to the four-day back trajectories reported by Bourtsoukidis et al. (2019), the measured air masses travelled to the northern part was from southern Europe and northeast Africa while the southern part was more influenced by air from the northern part of the Red Sea mixed with the air masses from desertic areas of central Africa. Therefore, less primary precursors as well as carbonyls were transported to the southern part of the Red Sea compared to the northern part. Moreover, the unexpected sources of hydrocarbons (ethane and propane) from Northern Red Sea deep water reported by Bourtsoukidis et al. (2020) would lead to higher carbonyl levels in the Northern part compared with the Southern part due to the additional precursors in the Red Sea North. However, acetaldehyde was still found to be significantly underestimated compared to the model results, even taking the deep-water source into consideration (section 3.3). This indicates that extra sources of acetaldehyde may exist, which will be discussed in detail in section 3.4.



280  
281  
  
  
282  
283  
284  
285  
286  
287  
288  
289  
290  
291  
292  
293

Table 1. Mean, standard deviation (SD) and median mixing ratios of aliphatic, unsaturated and aromatic carbonyls in different regions.

		Aliphatic Carbonyls								
		HCHO	CH3CHO	C3H6O	C4H8O	C5H10O	C6H12O	C7H14O	C8H16O	C9H18O
MS	mean	0.86	0.30	2.37	0.14	0.04	0.02	0.01	0.01	0.01
	SD	0.41	0.25	0.37	0.05	0.02	0.01	0.00	0.00	0.00
	median	0.80	0.25	2.32	0.12	0.03	0.02	0.01	0.01	0.01
Suez	mean	1.23	0.62	2.64	0.19	0.08	0.04	0.03	0.03	0.02
	SD	0.76	0.58	0.77	0.15	0.08	0.02	0.02	0.02	0.01
	median	1.11	0.42	2.52	0.13	0.04	0.04	0.02	0.03	0.02
RSN	mean	0.99	0.51	2.17	0.27	0.12	0.04	0.01	0.02	0.02
	SD	0.78	0.26	0.45	0.11	0.07	0.02	0.00	0.01	0.01
	median	0.73	0.46	2.17	0.25	0.10	0.04	0.01	0.02	0.02
RSS	mean	0.66	0.31	1.56	0.11	0.05	0.05	0.01	0.04	0.07
	SD	0.62	0.17	0.38	0.06	0.03	0.03	0.00	0.03	0.07
	median	0.40	0.26	1.60	0.09	0.04	0.05	0.01	0.03	0.04
GA	mean	0.69	0.19	0.81	0.04	0.03	0.04	0.02	0.02	0.02
	SD	0.33	0.08	0.27	0.02	0.01	0.02	0.01	0.01	0.01
	median	0.68	0.17	0.72	0.03	0.02	0.04	0.01	0.01	0.01
AS	mean	0.82	0.16	0.43	0.02	0.02	0.03	0.01	0.01	0.01
	SD	0.35	0.12	0.18	0.01	0.01	0.01	0.00	0.00	0.00
	median	0.86	0.13	0.34	0.02	0.02	0.04	0.01	0.01	0.01
GO	mean	1.27	0.26	1.33	0.10	0.08	0.04	0.01	0.02	0.02
	SD	0.59	0.12	0.40	0.06	0.04	0.03	0.00	0.01	0.01
	median	1.13	0.22	1.12	0.08	0.08	0.04	0.01	0.01	0.02
AG	mean	3.83	1.73	4.50	0.87	0.52	0.19	0.05	0.04	0.04
	SD	2.55	1.61	2.40	0.71	0.48	0.25	0.04	0.03	0.03
	median	3.02	1.02	3.77	0.56	0.31	0.10	0.04	0.03	0.03

		Aromatic Carbonyls			Unsaturated Carbonyls					
		C7H6O	C8H8O	C9H10O	C4H6O	C5H8O	C6H10O	C7H12O	C8H14O	C9H16O
MS	mean	0.04	0.02	0.01	0.02	0.02	0.02	0.01	0.02	-
	SD	0.03	0.01	0.00	0.03	0.02	0.01	0.00	0.00	-
	median	0.02	0.02	0.01	0.01	0.01	0.01	0.01	0.02	-
Suez	mean	0.13	0.04	0.03	0.07	0.05	0.05	0.03	0.02	0.01
	SD	0.23	0.05	0.01	0.08	0.05	0.04	0.02	0.01	0.00
	median	0.03	0.02	0.03	0.04	0.03	0.03	0.02	0.02	0.01
RSN	mean	0.10	0.07	0.03	0.03	0.04	0.05	0.03	0.02	0.02
	SD	0.10	0.06	0.03	0.02	0.03	0.03	0.02	0.01	0.01
	median	0.07	0.05	0.02	0.02	0.04	0.05	0.02	0.02	0.02
RSS	mean	0.08	0.09	0.04	0.02	0.03	0.04	0.02	0.06	0.03
	SD	0.07	0.07	0.03	0.01	0.02	0.03	0.01	0.11	0.02
	median	0.05	0.07	0.04	0.01	0.02	0.03	0.02	0.03	0.02
GA	mean	0.04	0.03	0.02	0.01	0.02	0.02	0.02	0.01	0.01
	SD	0.03	0.02	0.01	0.01	0.01	0.01	0.01	0.00	0.00
	median	0.02	0.02	0.02	0.01	0.02	0.02	0.01	0.01	0.01
AS	mean	0.03	0.02	0.01	0.01	0.02	0.02	0.01	0.01	0.01
	SD	0.04	0.01	0.00	0.01	0.01	0.01	0.00	0.00	0.00
	median	0.02	0.02	0.01	0.01	0.01	0.02	0.01	0.01	0.01
GO	mean	0.05	0.05	0.03	0.02	0.03	0.02	0.02	0.02	0.01
	SD	0.07	0.05	0.03	0.01	0.01	0.01	0.01	0.01	0.00
	median	0.03	0.03	0.02	0.02	0.03	0.02	0.02	0.01	0.01
AG	mean	0.15	0.13	0.05	0.07	0.11	0.12	0.06	0.04	0.03
	SD	0.15	0.10	0.04	0.07	0.11	0.10	0.05	0.03	0.02
	median	0.11	0.10	0.04	0.04	0.08	0.09	0.04	0.03	0.02

Table 2. Mixing ratios (ppb) of OVOCs reported in previous observation in literature

Locations	Lon./Lat.	Height	Time	Technique	Formaldehyde	Acetaldehyde	Acetone	MEK	Literature
<b>Open sea</b>		m							
Tropical Atlantic Ocean	10° N-0° N 35° W-5° E	18	Oct.-Nov.	PTR-MS	n.r.	n.r.	0.53	n.r.	(Williams et al., 2004)
Atlantic Ocean	50° N-50° S 10-60° W	18	Oct.-Nov.	PTR-MS	n.r.	0.18 (Northern H) 0.08 (Southern H)	0.6 (North) 0.2 (South)	n.r.	(Yang et al., 2014)
Western North Pacific Ocean	15-20° N 137° E	6.5 -14	May	PTR-MS	n.r.	n.r.	0.20-0.70	n.r.	(Tanimoto et al., 2014)
Western Indian Ocean	12° N-5° S 43-55° E	15	Feb.-Mar.	PTR-MS	n.r.	n.r.	0.49	n.r.	(Warneke and de Gouw, 2001)
Indian Ocean	19° N-13° S 67-75° E	10	Mar.	PTR-MS	n.r.	0.32-0.42 (continental outflow) 0.18-0.21 (equatorial marine)	1.11-2.08 (continental outflow) 0.51-0.62 (equatorial marine)	n.r.	(Wisthaler, 2002)
Southern Indian Ocean	30° S-49° S 30-100° E	15	Dec.	PTR-MS	n.r.	0.12-0.52	0.42-1.08	n.r.	(Colomb et al., 2009)
<b>Costal</b>									
Caribbean Sea	10-30° N 60-80° W	10	Oct.	HPLC	0.61	0.57	0.40	0.03	(Zhou and Mopper, 1993)
Cape Verde Atmospheric Observatory	16.86° N 24.87° W	10	2006 - 2011	GC-FID	n.r.	0.43 (0.19-0.67)	0.55 (0.23-0.91)	n.r.	(Read et al., 2012)
Appledore Island, USA	42.97° N 70.62° W	5	Jul.-Aug.	PTR-MS	n.r.	0.40	1.5	0.20	(White et al., 2008)
Mace Head, Ireland	53.3° N 9.9° W	25	Jul.-Sep.	GC-FID	n.r.	0.44 (0.12-2.12)	0.50 (0.16-1.67)	n.r.	(Lewis et al., 2005)
Canadian Archipelago	68-75° N 60-100° W	Ship cruise	Aug.-Sep.	PTR-MS	n.r.	n.r.	0.34	n.r.	(Sjostedt et al., 2012)
Barrow Arctic	71.30° N 156.77° W	6	Mar.-Apr.	TOGA		0.10 ± 0.20	0.90 ± 0.30	0.19 ± 0.05	(Hornbrook et al., 2016)
South China Sea, Sulu Sea	2° N-15° N 108-124° E	10	Nov.	GC-MS	n.r.	0.86	2.1	0.06	(Schlundt et al., 2017)
<b>Oil &amp; Gas</b>									
Horse Pool site, Uintah Basin, USA		Ground site	2012 - 2013	PTR-MS	3.71	4.27	7.97	2.81	(Koss et al., 2015)
Central United State		<600	Mar.-April	ToF-CIMS	1.13 <sup>a</sup>	0.5	1.5	0.2	(Koss et al., 2017)
Eagle Mountain Lake site, Texas, USA		Ground site	June	PTR-MS	n.r.	n.r.	3.2 (1.2-6.7)	0.3 (0.09-0.85)	(Rutter et al., 2015)

Hickory, Pennsylvania, a, USA	Ground site	June	PTR-MS	n.r.	1.29 (0.28-2.03)	3.22 (1.45-4.99)	0.73 (0.4-0.97)	(Swarthout et al., 2015)
-------------------------------------	----------------	------	--------	------	---------------------	---------------------	--------------------	-----------------------------

n.r.: not reported in the literature.  
a: formaldehyde was measured by laser-induced fluorescence (LIF)

### 3.1.2 Case studies of polluted regions: the Arabian Gulf and Suez

The primary emission sources in the Arabian Gulf and Suez regions are quite different. While the Arabian Gulf is dominated by oil and gas operations, Suez is more influenced by ship emissions and urban areas (Bourtsoukidis et al., 2019). Carbonyl compounds were most abundant in these two areas. For further insight, we focused on a time series of selected trace-gases and their inter-correlations to better identify the sources of the major aliphatic carbonyls. Meanwhile, we calculated the OH exposure ( $[OH]\Delta t$ ) based on hydrocarbon ratios (Roberts et al., 1984; de Gouw et al., 2005; Yuan et al., 2012) for the polluted regions (Arabian Gulf and Suez) where primary emissions have been identified (Bourtsoukidis et al., 2019; Bourtsoukidis et al. 2020), to better understand the photochemical aging of the major carbonyls using the following equation:

$$[OH]\Delta t = \frac{1}{k_X - k_Y} \cdot \left( \ln \frac{[X]}{[Y]} \right)_{t=0} - \ln \frac{[X]}{[Y]} , \tag{Eq. (1)}$$

where X and Y refer to two hydrocarbon compounds with different rates of reaction with the OH radical (k). For this study, we chose toluene ( $k_{OH+toluene}$ :  $5.63E-12 \text{ cm}^3 \text{ molecule}^{-1} \text{ s}^{-1}$ ) and benzene ( $k_{OH+benzene}$ :  $1.22E-12 \text{ cm}^3 \text{ molecule}^{-1} \text{ s}^{-1}$ ) (Atkinson and Arey, 2003), because both compounds were measured by PTR-ToF-MS at high frequency and these values showed a good agreement with values measured by GC-FID (Figure S2). The approach detailed by Yuan et al. (2012) was applied to determine the initial emission ratio  $\frac{[X]}{[Y]}_{t=0}$  in those two regions by only including nighttime data of benzene and toluene. We obtained initial emission ratios (toluene to benzene ratio) of 1.38 for the Arabian Gulf and 2.12 for the Suez region. Koss et al. (2017) summarized the toluene to benzene ratios observed in various locations and showed that urban and vehicle sources tend to have higher toluene to benzene ratio (mean ~ 2.5) than the ratios of oil & gas sources (mean ~ 1.2). Therefore, the toluene to benzene ratios obtained for those two regions agreed well with other studies done with similar emissions sources. The corresponding correlation plots of toluene and benzene for those two regions can be found in Figure S3.

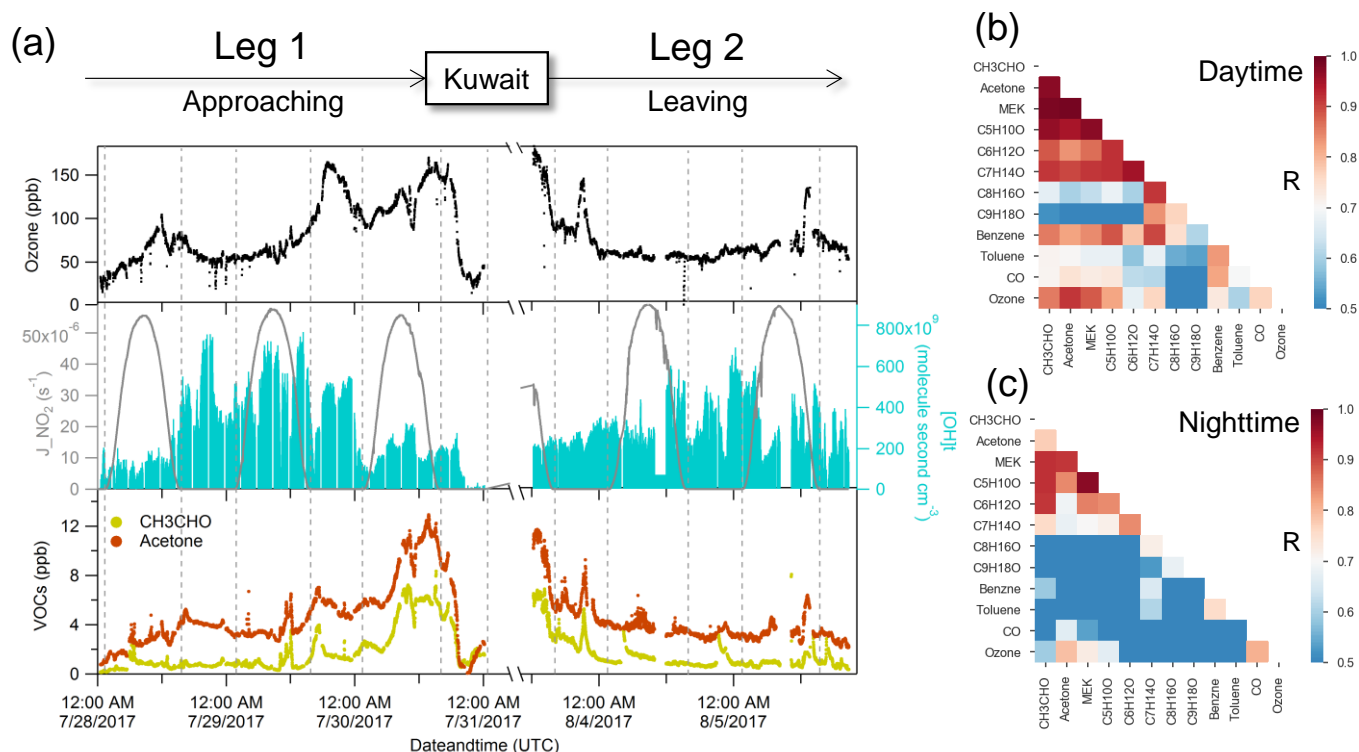


Figure 3. Case study of the Arabian Gulf. (a) Time series of selected species measured over the Arabian Gulf; (b) daytime correlation heat map of selected species; (c) nighttime correlation heat map of selected species.

Figure 3(a) shows the time series of acetaldehyde and acetone over the Arabian Gulf along with OH exposure ( $[OH]t$ ) and ozone. We further separated the data into daytime and nighttime and calculated correlations among the carbonyls and other selected species (see Fig. 4b and c). Aliphatic carbonyls were well correlated with each other during the daytime and ozone had a generally good correlation with C2-C7 carbonyls ( $r > 0.7$ ) during the daytime but a much lower correlation during the night, indicating ozone and carbonyls were co-produced via photochemical oxidation. Tadic et al. (2020) reported the net ozone production rate over the Arabian Gulf ( $32 \text{ ppb d}^{-1}$ ) was the greatest over the Arabian Peninsula. They show that strong ozone forming photochemistry occurred in this region, which would lead to abundant secondary photo-chemically produced products (including carbonyls). However, it should be noted the good correlation between ozone and carbonyls could in part be due to carbonyls co-emitted with ozone precursors (hydrocarbons) as primary emissions. In Figure 3 (a), the calculated OH exposure was high during the first night in leg 1, where an elevation of acetone mixing ratio was observed while the mixing ratio of acetaldehyde remained relatively constant. With limited OH radical abundance during the nighttime, the increased OH exposure indicates that the air reaching the ship was photochemically processed (aged). Therefore, the increase of acetone was mainly from long-distance transport as acetone has a much longer atmospheric lifetime than acetaldehyde. As the ship approached Kuwait, the calculated OH exposure was low (starting from 7/30/2017, 12:00 am UTC), which is an indicator of nearby emission sources. The lifetime of the OH radical derived from the measured OH reactivity also decreased from  $\sim 0.1 \text{ s}$  to  $\sim 0.04 \text{ s}$  during the same period (Pfannerstill et al., 2019). Oil fields and associated refineries are densely distributed in the northwest of the Arabian Gulf region (United States Central Intelligence Agency). The air reaching the ship when mixing ratios of acetone and acetaldehyde were highest was mainly from the Northwest (Iraq oil field region) according to the back trajectories (Bourtsoukidis et al., 2019). This suggests that the air masses encountered in Northwest Arabian Gulf were a combination of fresh emissions from nearby sources and photochemically processed

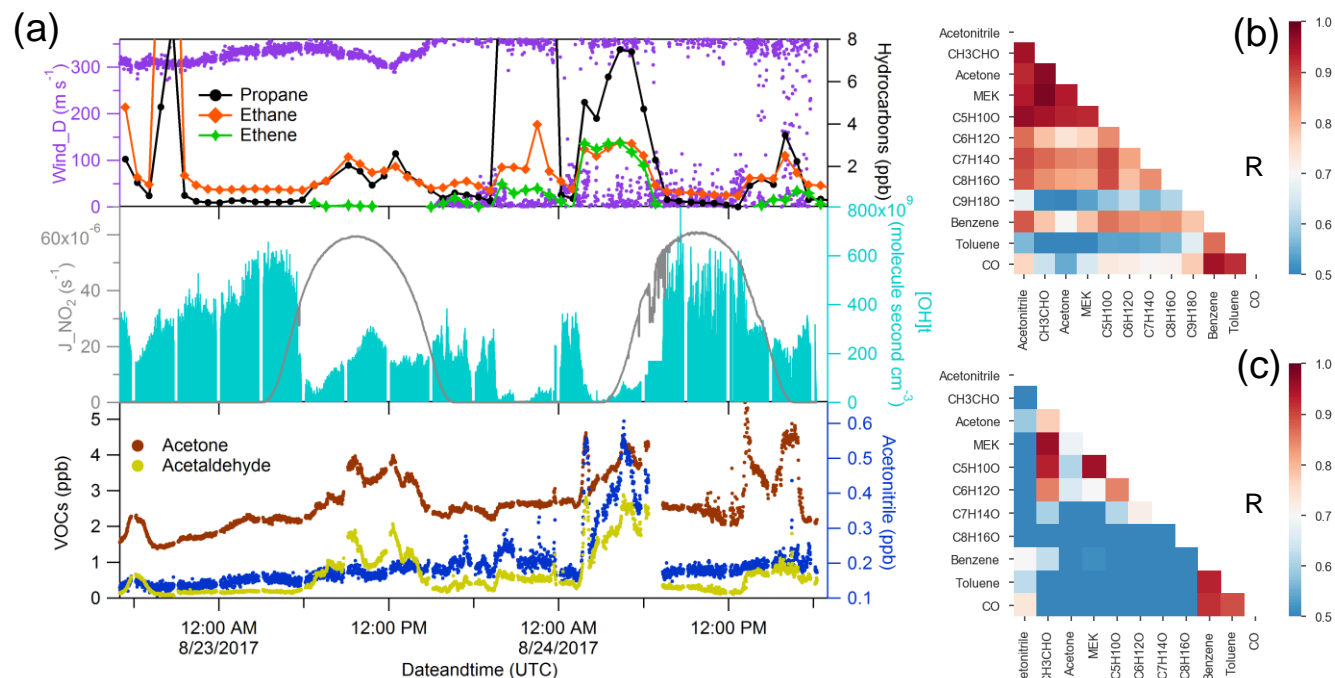


Figure 4. Case study of Suez. (a) Time series of selected species measured over Suez; (b) correlation heat map of selected species during biomass burning plume (UTC 01:00 -06:00 August 24<sup>th</sup> 2017); (c) correlation heat map of selected species without the period of biomass burning plume.

For the Suez region (Gulf of Suez and Suez Canal), data were only available for the second leg. A significant increase of acetonitrile (over 400 ppt) was observed just before entering the Great Bitter Lake (see Figure 4a), indicating an increasing influence of biomass burning on the air composition (Lobert et al., 1990). Carbonyl compounds are important primary emissions in fresh biomass burning plumes (Holzinger et al., 1999;Schauer et al., 2001;Holzinger et al., 2001;Koss et al., 2018) as well as being formed as secondary products in more aged plumes (Holzinger et al., 2005). We further investigated the correlation coefficient among carbonyls during the biomass burning plume (Figure 4b) in Suez. Carbonyls had a high correlation with acetonitrile, benzene and among themselves, particularly for smaller carbonyls (acetaldehyde, C<sub>3</sub>-C<sub>5</sub> carbonyls). The biomass burning emissions were probably transported by on the prevailing northerly wind (Figure S1) above Northeast Egypt where crop residues especially rice straw is often directly burned in the open fields (Abdelhady et al., 2014;Said et al., 2013;Youssef et al., 2009). Besides the direct biomass burning emission, the high mixing ratios and the good correlations of carbonyls could also have resulted from other sources as hydrocarbons (alkanes, alkenes and aromatics) which were elevated at the same time. Similar to conditions identified over the Arabian Gulf, elevated OH exposure accompanied with increasing acetone mixing ratio was observed during the first night over the Gulf of Suez, indicating aged air mass transportation. The OH exposure was then significantly lower during the daytime, when mixing ratios of carbonyls and alkanes increased as well. This indicates the presence of emission sources nearby.

Oil refineries located in the coastal side of Suez and oil tank terminals located in the northern part of the Gulf of Suez are likely sources.

## **3.2 Unsaturated and aromatic carbonyls ( $C_nH_{2n-2}O$ ), ( $C_nH_{2n-8}O$ )**

### **3.2.1 Overview**

The mixing ratios of unsaturated carbonyls were generally low with values below 30 ppt over the Mediterranean Sea and the clean regions (the Arabian Sea and the Gulf of Aden, 12 - 21 ppt). The Red Sea region and the Gulf of Oman had slightly higher levels (13 – 60 ppt). The highest values were again observed in the Arabian Gulf (25 – 115 ppt) followed by Suez (11 – 68 ppt). The numbers represent the range of the mean mixing ratios of unsaturated carbonyls in each region. In terms of the mixing ratio distribution (Figure 2), the peak value was usually observed at C5 or C6 unsaturated carbonyls over most regions except for Suez where C4 carbonyl had the highest mixing ratio. Based on chemical formulas, unsaturated carbonyls can be either cyclic carbonyl compounds or carbonyls containing a carbon-carbon double bond. Therefore, the air chemistry could differ considerably depending on the compound assignment. A detailed analysis of the chemistry of the unsaturated carbonyls measured will be given in the following section 3.2.2.

Regional variability was also observed for aromatic carbonyls with highest levels observed over the Arabian Gulf and Suez, and much lower mixing ratios over the Arabian Sea, Mediterranean Sea and Gulf of Aden (Table 1). Several studies using PTR-MS have reported values for m/z 107.049 (C7 aromatic carbonyls) attributed to benzaldehyde (Brilli et al., 2014; Koss et al., 2017; Koss et al., 2018), m/z 121.065 (C8 aromatic carbonyls) attributed to tolualdehyde (Koss et al., 2018) or acetophenone (Brilli et al., 2014) and m/z 135.080 (C9 aromatic carbonyls) attributed to methyl acetophenone (Koss et al., 2018) or benzyl methyl ketone (Brilli et al., 2014) or 3,5-dimethylbenzaldehyde (Müller et al., 2012). Atmospheric aromatic carbonyls are produced via photochemical oxidation of aromatic hydrocarbons (Finlayson-Pitts and Pitts Jr, 1999; Wyche et al., 2009; Müller et al., 2012) and benzaldehyde was reported as having primary sources from biomass burning and anthropogenic emissions (Cabrera-Perez et al., 2016). Around the Arabian Peninsula, the level of aromatic carbonyls declined with increasing carbon number over most of the regions except in the Red Sea South where C8 carbonyls were slightly higher than C7 (Figure 2). Interestingly, only in the Suez region, were the C7 aromatic carbonyls more abundant than other aromatic carbonyls, whereby the mean value ( $128 \pm 229$  ppt) was much higher than the median value (30 ppt), indicating strong primary sources of benzaldehyde in Suez. Otherwise, toluene was found to be more abundant over Suez with mean mixing ratios of  $271 \pm 459$  ppt than over other regions (the mean over the Arabian Gulf:  $130 \pm 160$  ppt) which would also lead to higher benzaldehyde as it is one of the OH-induced oxidation products of toluene via H-abstraction (Ji et al., 2017).

### **3.2.2 Potential precursors and sources of unsaturated carbonyls**

Unsaturated carbonyls measured by PTR-MS have been only rarely reported in the atmosphere with the exception of methyl vinyl ketone and methacrolein (C4 carbonyls) which are frequently reported as the oxidation products of isoprene (Williams et al., 2001; Fan and Zhang, 2004; Wennberg et al., 2018). According to the GC-FID measurement, isoprene was below the detection limit for most of the time during the AQABA cruise with the highest values observed in Suez (10 - 350 ppt). This shows that the AQABA campaign was little influenced by either terrestrial or marine isoprene emissions. However, we observed unexpected high levels on mass 69.070, which is usually interpreted as isoprene for PTR-MS measurements. Significant enhancements were even identified while sampling our own ship exhaust (in PTR-MS but not GC-FID), suggesting the presence of an anthropogenic interference at that mass under these extremely polluted conditions. Several studies have reported possible fragmentations of cyclic

alkanes giving mass ( $m/z$ ) 69.070. These include: a laboratory study on gasoline hydrocarbon measurements by PTR-MS (Gueneron et al., 2015), a GC-PTR-MS study of an oil spill site combined with analysis of crude oil samples (Yuan et al., 2014) and an inter-comparison of PTR-MS and GC in an O&G industrial site (Warneke et al., 2014). From those studies, other fragmentations from C5-C9 cycloalkanes including  $m/z$  43,  $m/z$  57,  $m/z$  83,  $m/z$  111 and  $m/z$  125 were identified together with  $m/z$  69. Cyclic alkanes were directly measured in oil and gas fields (Simpson et al., 2010; Gilman et al., 2013; Li et al., 2017; Aklilu et al., 2018), vehicle exhaust (Gentner et al., 2012; Erickson et al., 2014), vessel exhaust (Xiao et al., 2018), accounting for a non-negligible amount of the total VOCs mass depending on the fuel type. Koss et al. (2017) reported enhancement of cyclic alkane fragment signals and increased levels of unsaturated carbonyls measured by PTR-ToF-MS over O&G region in the US. The unsaturated carbonyls (C5-C9) were assigned as oxidation products of cycloalkanes. Therefore, we examined the correlations between  $m/z$  69.070 and other cycloalkane fragments over the Arabian Gulf and Suez, where anthropogenic primary emissions were significant. As shown in Figure 5,  $m/z$  83 was the most abundant fragment and it correlated better with  $m/z$  69 than the other two masses, strongly supporting the presence of C6 cycloalkanes (methylcyclopentane and cyclohexane). The other two masses are distributed in two or three clusters, suggesting compositions of different cycloalkanes.  $M/z$  43 and  $m/z$  57 (fragments of C5 cycloalkanes) had lower correlations with other fragments (not shown in the graph) as they are also fragments of other higher hydrocarbons. Thereby we could assign those unsaturated carbonyls as photochemical oxidation products (i.e. cyclic ketones or aldehydes) from their precursor cycloalkanes.

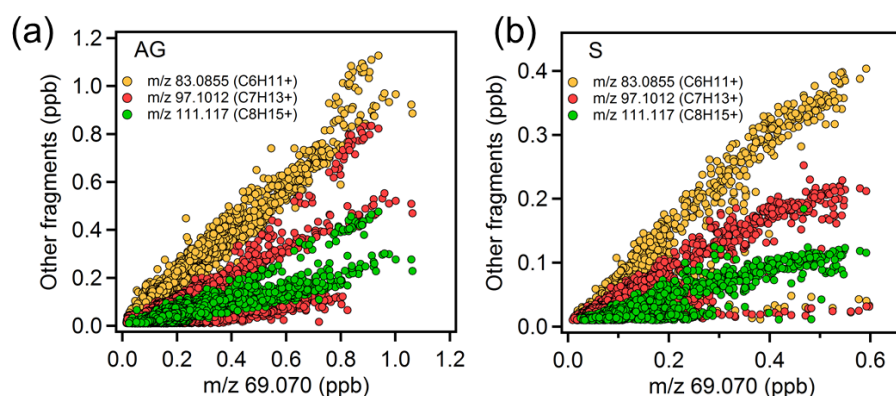


Figure 5. Scatter plots of  $m/z$  69.070 and other cycloalkane fragment masses over the (a) Arabian Gulf and (b) Suez region.

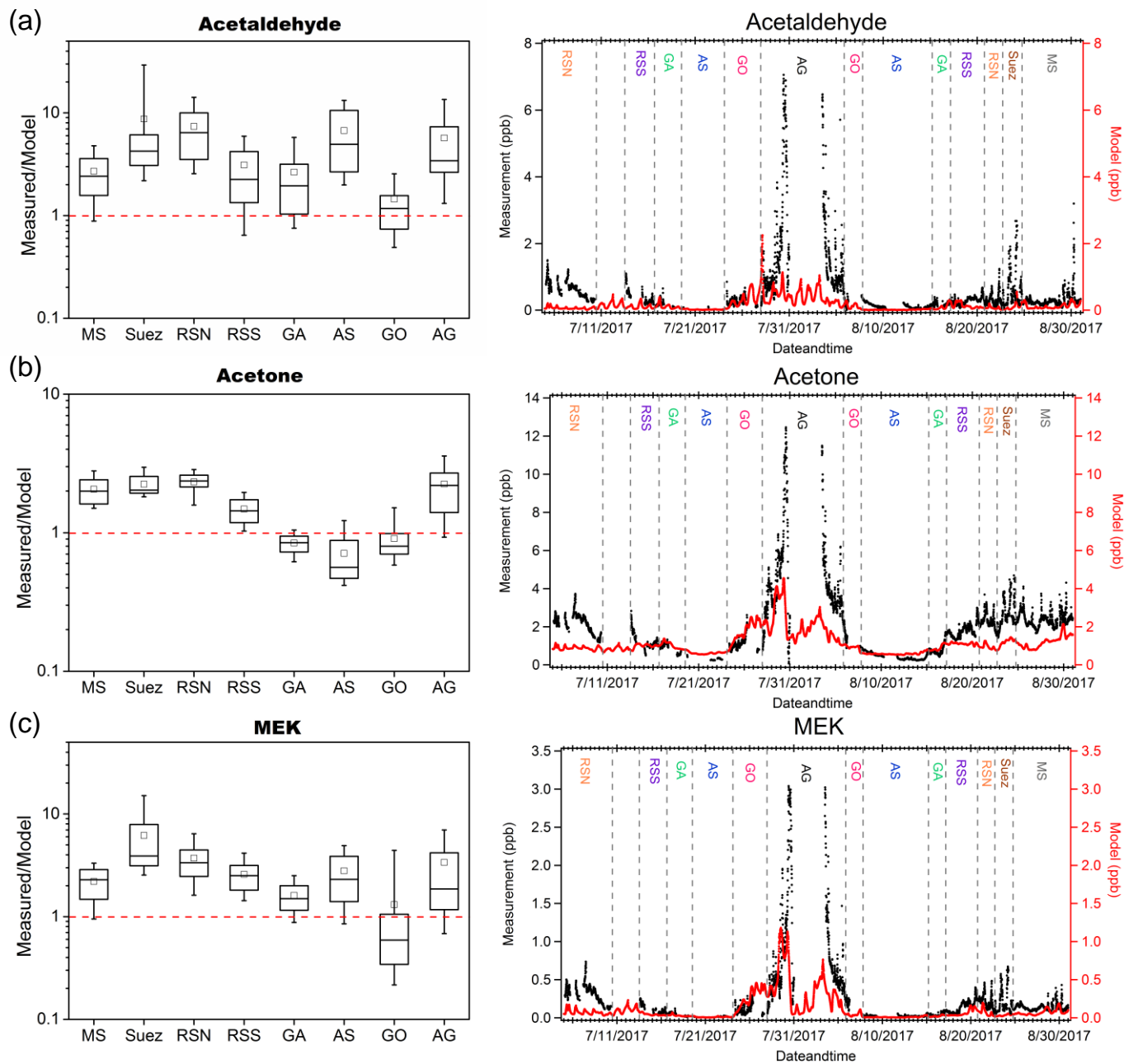
As shown in Figure 2 and Table 1, C6 unsaturated carbonyls displayed higher mixing ratios than any other unsaturated carbonyls over the Arabian Gulf while C5 unsaturated carbonyl was slightly higher than C6 in Suez. Bourtsoukidis et al. (2019) derived enhancement ratio slopes from pentane isomers and established that the Arabian Gulf is dominated by oil and gas operations and that Suez is more influenced by ship emissions. Therefore, as the Arabian Gulf had much more active O&G activities than Suez, our findings agree with Koss et al. (2017) who showed that C6 unsaturated carbonyls should be more abundant than C5 carbonyls since more precursors for C6 unsaturated carbonyls are emitted from active oil fields. It is worth mentioning that in Figure 5 (b) one cluster at the bottom showed  $m/z$  69.070 had no correlation with other three masses. Those points correspond to the time when the GC measured significant elevated isoprene while passing through the narrow Suez Canal where some vegetation (e.g. palms and some agriculture) was present close to shore, meaning  $m/z$  69.070 during this period was isoprene. At the same time,  $m/z$  71.049 (C4 unsaturated carbonyl) increased from 20 ppt to 220 ppt. Isoprene oxidation products (MVK and methacrolein) were probably the major contribution to the C4 unsaturated carbonyls in this period. This also explains why C4 carbonyl dominated the distribution of unsaturated carbonyls over Suez.



445 In the other regions (especially more remote areas), the cyclic alkane fragmentation masses had much lower abundance, leading  
446 to much less unsaturated carbonyls due to lack of precursors. Meanwhile,  $m/z$  69.070 ( $C_5H_8H^+$ ),  $m/z$  83.086 ( $C_6H_{10}H^+$ ) and  $m/z$   
447 97.101 ( $C_7H_{12}H^+$ ) could also be fragmentations from corresponding aldehydes losing one water molecule as mentioned in section  
448 2.3.3. Missing information of the chemical structure of unsaturated carbonyls and knowledge of their precursors, preclude detailed  
449 investigation of the sources of large unsaturated carbonyls in these areas.

### 450 3.3 Model comparison of acetaldehyde, acetone and MEK

451 We compared our measurement results of acetaldehyde, acetone and MEK to those predicted by the global model “EMAC”  
452 (ECHAM5/MESSy2 for Atmospheric Chemistry). From the results shown in Figure 6, the model predicted acetone much better  
453 than acetaldehyde and MEK. In general, the model broadly captured the major features identified during the campaign such as  
454 much higher levels of carbonyls mixing ratios over the Arabian Gulf and Suez and relatively low levels over the Arabian Sea. The  
455 mean measurements-to-model ratios indicated that acetone was overestimated by a factor within 1.5 over the Arabian Sea, Gulf of  
456 Aden and Gulf of Oman, and underestimated by a factor within 2.5 over the other regions. In contrast, the model underestimated  
457 MEK within a factor of 4 over most of the regions except for the Gulf of Oman where MEK was overestimated (median values  
458 were taken here as the mean values substantially deviated from the medians over Suez, Gulf of Oman and Arabian Gulf). The  
459 model underestimation was most significant for acetaldehyde, which is underpredicted by a factor (median values) of more than 6  
460 over the Red Sea North, ~ 4 over the Arabian Sea and Arabian Gulf and between 1 and 4 over other regions. A strong natural non-  
461 methane hydrocarbon source from deep water in the Northern Red Sea was implemented in the model (Bourtsoukidis et al., 2020).  
462 Although the model representation of acetaldehyde and other carbonyls was clearly improved after including the deep water source  
463 of ethane and propane (Figure S4), the underestimation of acetaldehyde was still significant over the Red Sea North as shown in  
464 Figure 6(a), indicating further missing sources. For acetaldehyde and MEK, the discrepancy was also significant over the Arabian  
465 Sea where acetone was in contrast, overestimated. Since acetaldehyde had the biggest bias from the model prediction, we further  
466 investigate the possible missing sources of acetaldehyde.



468

469 Figure 6. Measurement to model ratios (left) and time series (right) of measurements (in black) and model simulation (in red) of  
470 (a) acetaldehyde; (b) acetone; (c) MEK in each area. In each box plot, the box represents 25% to 75% of the data set with central  
471 line and square indicating the median value and the mean value respectively. The whiskers show data from 10% to 90%. The red  
472 dashed lines represent the 1:1 ratio.

### 473 3.4 Missing sources of acetaldehyde

474 In this section we investigate the following processes as potential sources of acetaldehyde: (1) production as an inlet artifact, (2)  
475 oceanic emission of acetaldehyde, (3) anthropogenic primary sources, (4) biomass burning sources, and (5) other possible  
476 secondary formation pathways.

#### 477 3.4.1 Inlet artifact

Northway et al. (2004) and Apel et al. (2008) reported that heterogeneous reactions of unsaturated organic species with ozone on the wall of the Teflon inlet can cause artifacts signal of acetaldehyde but not to acetone. During AQABA, the highest and the most variable ozone mixing ratios were observed during the campaign over the Arabian Gulf (mean:  $80 \pm 34$  ppb) and the Red Sea North ( $66 \pm 12$  ppb), where a modest correlation was found between acetaldehyde and ozone over the Arabian Gulf ( $r^2=0.54$ ) and no significant correlation over the Red Sea North ( $r^2=0.40$ ). However larger correlation coefficients were identified between ozone and other carbonyls over the Arabian Gulf (see Figure S5), which suggests that the correlation was due to atmospheric photochemical production rather than artifacts. Moreover, acetaldehyde was found to have a much worse correlation with ozone during the nighttime compared to the correlation during the daytime over the Arabian Gulf (Figure 3b and c), which also indicates that inlet generation of acetaldehyde was insignificant. Over other regions, especially the remote area (the Arabian Sea and Gulf of Aden), ozone was relatively constant and low, with poor correlation with acetaldehyde mixing ratios. Although we cannot completely exclude the possible existence of artifacts, the interference is likely to be insignificant in this dataset.

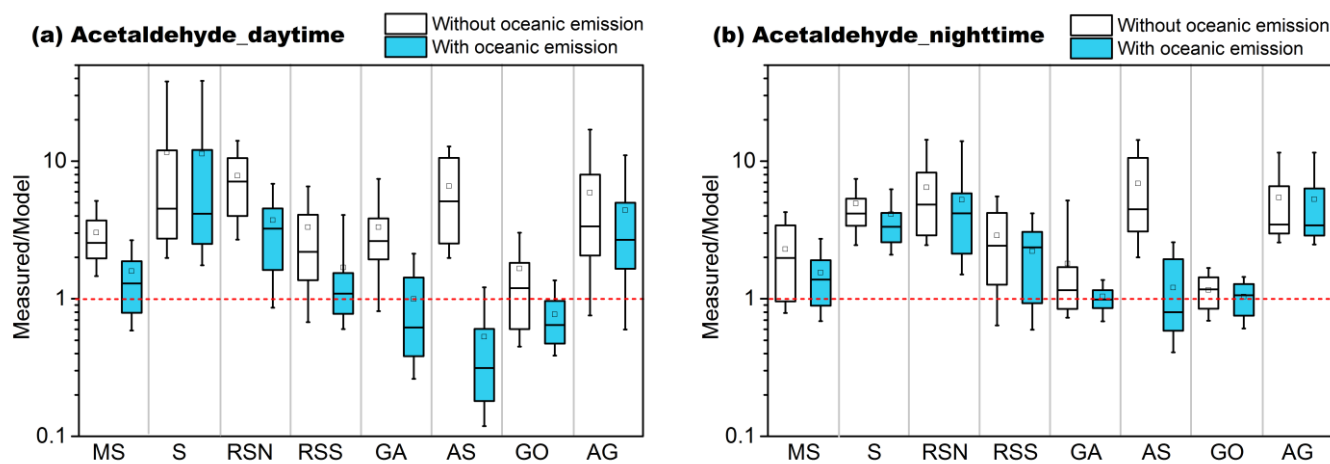
### 3.4.2 Oceanic emission

A bias between measured acetaldehyde and global model simulations has been observed in previous studies conducted in the remote troposphere (Singh et al., 2003; Singh, 2004; Wang et al., 2019) and in the marine boundary layer (Read et al., 2012). The aforementioned studies emphasized the potential importance of the sea water acting as a source of acetaldehyde emission via air-sea exchange. No significant correlation was found between acetaldehyde and DMS, a marker of marine biogenic emission which is produced by phytoplankton in seawater (Bates et al., 1992) (see Figure S6). This indicates that the direct biogenic acetaldehyde emissions from the ocean are probably insufficient to explain the measured acetaldehyde. More likely, acetaldehyde and other small carbonyl compounds can be formed in the sea especially in the surface microlayer (SML) via photodegradation of colored dissolved organic matter (CDOM) (Kieber et al., 1990; Zhou and Mopper, 1997; Ciuraru et al., 2015). Zhou and Mopper (1997) calculated the exchange direction of small carbonyls based on measurement results and identified that the net flux of acetaldehyde was from sea to the air whereas formaldehyde was taken up by the sea. Sinha et al. (2007) characterized air-sea flux of several VOCs in a mesocosm experiment and found that acetaldehyde emissions were in close correlation with light intensity ( $r=0.7$ ). By using a 3-D model, Millet et al. (2010) estimated the net oceanic emission of acetaldehyde to be as high as  $57 \text{ Tg a}^{-1}$  (in a global total budget:  $213 \text{ Tg a}^{-1}$ ), being the second largest global source. A similar approach was applied in a recent study done by Wang et al. (2019), reporting the upper limit of the net ocean emission of acetaldehyde to be  $34 \text{ Tg a}^{-1}$ . Yang et al. (2014) quantified the air-sea fluxes of several OVOCs over Atlantic Ocean by eddy covariance measurements, showing ocean is a net source for acetaldehyde. Although Schlundt et al. (2017) reported uptake of acetaldehyde by the ocean from measurement-inferred fluxes in western Pacific coastal regions, to our knowledge, there is no direct experimental evidence showing the ocean to be a sink for acetaldehyde.

In order to test the importance of the oceanic emission of acetaldehyde, we implemented this source in EMAC model. The measured sea water concentration of acetaldehyde was not available for the water area around the Arabian Peninsula. Wang et al. (2019) estimated the global average acetaldehyde surface seawater concentrations of the ocean mixed layer using a satellite-based approach similar to Millet et al. (2010), where the model estimation agreed well with limited reported measurements. From the Wang et al. (2019) results, the averaged seawater concentration of acetaldehyde around Arabian Peninsula was generally much higher from June to August. As the photodegradation of CDOM is highly dependent on sunlight, the air-sea submodel (Pozzer et al., 2006) was augmented to include throughout the campaign a scaled acetaldehyde seawater concentration in the range of  $0 \sim 50 \text{ nM}$  according to the solar radiation (Figure S7). With this approach, the average of acetaldehyde seawater concentration estimated by the model is  $13.4 \text{ nM}$ , a reasonable level compared to predicted level by Wang et al. (2019).

517 After adding the oceanic source of acetaldehyde, the model estimation was significantly improved (Figure 7). As the oceanic source  
 518 in the model is scaled according to the solar radiation, the measurement-to-model ratios were more strongly reduced during the  
 519 day compared to the night. With oceanic emission included, the model underestimation was less significant, within a factor of 3  
 520 during the day and 4 during the night over the Mediterranean Sea, Red Sea and Gulf of Aden. The most significant improvement  
 521 was identified over the Red Sea North. As shown in Figure 8, the model had much better agreement with the measurement after  
 522 adding the oceanic source. The scatter plots for other regions can be found in Figure S8. Over the Arabian Sea, the model  
 523 significantly overestimated acetaldehyde mixing ratios, indicating the input sea water concentration of acetaldehyde might be too  
 524 high. The SML layer starts to be effectively destroyed by the wave breaking when the wind speed exceeds than  $8 \text{ m s}^{-1}$  (Gantt et  
 525 al., 2011). As the average wind speed over the Arabian Sea was the highest among the cruised areas ( $8.1 \pm 2.4 \text{ m s}^{-1}$ , Figure S1),  
 526 less contribution from the CDOM photo degradation to acetaldehyde in the surface sea water would be expected. For the Suez  
 527 region, due to the limited model resolution ( $1.1^\circ \times 1.1^\circ$ ), little sea water was identified in the model, leading to negligible influence  
 528 from the oceanic source.

529 Model underestimation of acetaldehyde especially over the Suez, Red Sea and Arabian Gulf is also likely to be related to the coarse  
 530 model resolution ( $\sim 1.1^\circ \times 1.1^\circ$ ) (Fischer et al., 2015). Where model grid points contain areas of land the higher and more variable  
 531 terrestrial boundary layer height impacts the model prediction whereas the measurements may only be influenced by a shallower  
 532 and more stable marine boundary layer.



533  
 534 Figure 7. Acetaldehyde measurement to model ratios without the oceanic source (white boxes) and with the oceanic source (blue  
 535 boxes) in the model during (a) daytime and (b) nighttime in different regions. The boxes represent 25% to 75% of the data set  
 536 with the central line and square indicating the median and mean values, respectively. The whiskers show data from 10% to 90%.  
 537 The red dashed lines represent the 1:1 ratio.

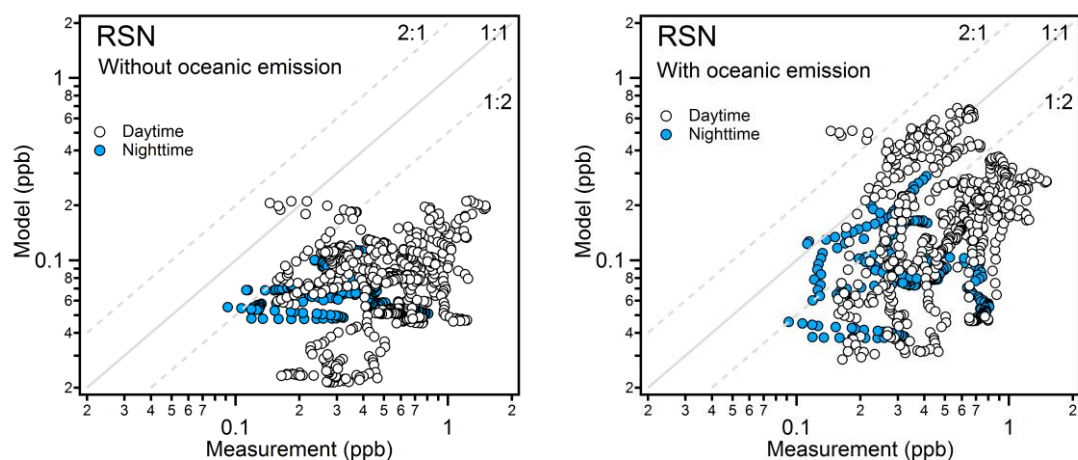


Figure 8. Observed and simulated mixing ratios of acetaldehyde over the Red Sea North without oceanic emission (left) and with oceanic emission (right). The data points are separated into day- and nighttime according to solar radiation.

### 3.4.3 Anthropogenic primary sources

Over the Arabian Gulf and Suez, the intensive photochemical production of carbonyls is apparent. Bourtsoukidis et al. (2020) compared measured hydrocarbons (ethane, propane, and butane) with the results from model simulations (the same model used in this study with the newly discovered deep water source implemented). The model was able to reproduce the measurement over most regions except for some significant model underestimations in Suez and Arabian Gulf, in which local and small-scale emissions were difficult for the model to capture. Therefore, an underestimation of the precursor hydrocarbons, as well as those large alkanes, alkenes and cyclic hydrocarbons which were not measured ( $> C_8$ ) or included in the model ( $> C_5$ ) could be a reason for the model underestimation of acetaldehyde especially in polluted regions. In addition, as mentioned in the previous case studies, high ozone mixing ratios were observed over the Arabian Gulf especially during the nighttime. Ethene and propene were found to be significantly underestimated during the nighttime high ozone period by a factor over 10 (Figure S9), which indicates that the nighttime ozonolysis of alkenes could be another important source for acetaldehyde, formaldehyde and other carbonyls (Atkinson et al., 1995; Altshuler, 1993) in the Arabian Gulf.

Acetaldehyde, an oxygenated VOC, is not generally considered as an important primary emission from oil and gas field but instead a photochemical product of hydrocarbon oxidation (Yuan et al., 2014; Koss et al., 2015; Koss et al., 2017). In contrast, primary sources of formaldehyde from oil and gas production processes including both combustion and non-combustion process have been ascertained (Vaught, 1991). Le Baron and Stoeckenius (2015) concluded in their report of the Uinta Basin winter ozone study that besides formaldehyde, the other carbonyls were poorly understood in terms of their primary sources. Acetaldehyde and other carbonyls (aldehydes and ketones) have been reported as primary emissions from fossil fuel combustion including ship emissions (Reda et al., 2014; Xiao et al., 2018; Huang et al., 2018) and vehicle emissions (Nogueira et al., 2014; Erickson et al., 2014; Dong et al., 2014). A possible explanation for the measurement-model discrepancy is that the active petroleum industry located in the Arabian Gulf and intensive marine transportation in Suez are primary sources of acetaldehyde and other carbonyls which were not well constrained in the model. The Suez region, where the largest acetaldehyde discrepancy was identified, had a significant influence from biomass burning (see section 3.2.2). Biomass burning emissions are notoriously difficult to model as they are highly variable both in time and space. In this study, the model failed to reproduce the acetonitrile level with a range of only 40-50 ppt rather than 100-550 ppt measured over Suez. Thus, besides the possibility of seawater emission from the Gulf of Suez and the Suez Canal, the underestimated biomass burning source in the model over Suez, will lead to an underestimation of acetaldehyde as well as other carbonyl compounds in this region.

#### 568 3.4.4 Other possible secondary formation pathways

569 Although the model estimation was generally improved with the addition of an oceanic source, the model to measured ratios still  
570 varied over a wide range. As mentioned above, photodegradation of CDOM on the surface of seawater is a known source for  
571 acetaldehyde although some studies focusing on real sea water samples did not observe clear diel cycles of seawater acetaldehyde  
572 (Beale et al., 2013; Yang et al., 2014). Fast microbial oxidation could be a reason (Dixon et al., 2013) while other non-light driven  
573 sources of acetaldehyde could be an alternative explanation. In a recent study, Zhou et al. (2014) reported enhanced gas-phase  
574 carbonyl compounds including acetaldehyde during a laboratory experiment of ozone reacting with SML samples, indicating  
575 acetaldehyde could also be produced under non-light driven heterogeneous oxidation. Wang et al. (2019) ventured a hypothetical  
576 source that organic aerosol can be an extra source for unattributed acetaldehyde in the free troposphere through light-driven  
577 production and ozonolysis. However, since the yield of acetaldehyde from such reactions is unknown, large uncertainties remain.  
578 Previous studies have shown that the organic matter fraction was highest in smaller sea spray aerosols and that the aerosols contain  
579 both saturated and unsaturated fatty acids originating from the seawater surface (i.e. SML) (Mochida et al., 2002; Cochran et al.,  
580 2016). Thus, for the AQABA campaign, both photodegradation and heterogeneous oxidation could occur on the surface of sea  
581 spray and pollution associated aerosols, even over remote open ocean therefore being an extra source of acetaldehyde and other  
582 carbonyl compounds.

583 Another acetaldehyde formation pathway reported is gas-phase photolysis of pyruvic acid (Eger et al., 2019b; Reed Harris et al.,  
584 2016), a compound mainly of biogenic origin. Pyruvic acid has been also observed in seawater (Kieber and Mopper, 1987; Zhou  
585 and Mopper, 1997) and was found up to 50 nM in the surface water of eastern Pacific Ocean (Steinberg and Bada, 1984), while  
586 acetaldehyde was not the major product of aqueous-phase photolysis of pyruvic acid (Griffith et al., 2013). Zhou and Mopper  
587 (1997) pointed out that the net exchange direction for pyruvic acid is expected to be from the air to the sea due to high solubility,  
588 with Henry's law constant of  $3.1 \times 10^3 \text{ mol m}^{-3} \text{ Pa}^{-1}$  (Sander, 2015). Moreover, partitioning to aerosols could be an important sink  
589 for pyruvic acid (Reed et al., 2014; Griffith et al., 2013): an increasing concentration trend of pyruvic acid was observed in marine  
590 aerosols over western North Pacific Ocean (Boreddy et al., 2017). Therefore, due to limited terrestrial biogenic sources of pyruvic  
591 acid for AQABA campaign, gas-phase level of pyruvic acid was expected to be low. Limited studies reported pyruvic acid level  
592 in marine boundary layer, Baboukas et al. (2000) measured  $1.1 \pm 1.0$  ppt of pyruvic acid above Atlantic Ocean. Pyruvic acid was  
593 measured by Jardine et al. (2010) using a PTR-MS at  $m/z$  89 in a forested environment. For the AQABA PTR-ToF-MS data set,  
594 enhanced signals were observed at  $m/z$  89.024 with the mean mixing ratio of 35-110 ppt over different regions (Table S4), which  
595 is much more abundant than reported pyruvic acid levels by Baboukas et al. (2000). This might be due to the uncertainty associated  
596 with the theoretical methods of quantification used here or the presence of isomeric compounds on that mass, since pyruvic acid  
597 was not calibrated with the standard. Even if we assume the  $m/z$  89.024 to be entirely pyruvic acid, with 60% yield of acetaldehyde  
598 via photolysis (IUPAC, 2019), it gave maximum 13 ppt of acetaldehyde over Arabian Gulf, 5-9 ppt over other regions, which were  
599 only 0.8% - 6% of the mean mixing ratios (Table S4). Detailed information of the calculation can be found in the Supporting  
600 Information. Therefore, we conclude that the contribution from the photolysis of pyruvic acid is not an important source for the  
601 unattributed acetaldehyde during the AQABA campaign.

#### 602 4 Summary and Conclusion

603 Observations of carbonyl compounds around the Arabian Peninsula were investigated in terms of mixing ratios abundance over  
604 different areas. Aliphatic carbonyl compounds were generally more abundant than the unsaturated and aromatic carbonyl  
605 compounds, and were dominated by low-molecular-weight compounds (carbon number less than five). Aliphatic carbonyl

606 compounds were found at the highest mixing ratios over the Arabian Gulf followed by the Suez region, while the lowest mixing  
607 ratios were observed over the Arabian Sea and the Gulf of Aden. Over the Mediterranean Sea, aliphatic carbonyls were low except  
608 for acetone that was much higher compared to the levels observed over clean remote areas (i.e. Arabian Sea). The atmospheric  
609 composition over the Red Sea showed obvious differences between the northern and the southern part, with higher mixing ratios  
610 in the north. Similar region-dependent distributions were observed for unsaturated and aromatic carbonyls. Generally, the mixing  
611 ratios of aromatic carbonyl compounds decreased as the carbon number increased. Particularly over the Suez region, benzaldehyde  
612 (C7 aromatic carbonyls) was much more abundant than other aromatic carbonyls, indicating direct sources as well as abundant  
613 oxidation precursors. For unsaturated carbonyl compounds, C5 and C6 carbonyl compounds dominated the mixing ratio  
614 distribution, while the air chemistry highly depends on the chemical structure assignment of those masses.

615 Further case studies showed that the carbonyl compounds were highly correlated to the high ozone levels during daytime over the  
616 Arabian Gulf while the air chemistry in Suez region was strongly influenced by regional biomass burning. Due to the unexpectedly  
617 high loading of m/z 69 (usually assigned as isoprene) observed in highly polluted regions, we further identified the correlations  
618 between m/z 69 and other fragmentation masses of cycloalkanes according to previous studies conducted in oil and gas regions  
619 (Warneke et al., 2014; Yuan et al., 2014; Koss et al., 2017). The high correlations among fragments implied the existence of  
620 cycloalkanes in the polluted regions, which could be further oxidized to unsaturated carbonyl compounds (cyclic ketones or  
621 aldehydes).

622 As acetaldehyde was identified as having important additional sources, we further compared the measurements of major carbonyl  
623 species (acetaldehyde, acetone and MEK) with a comprehensive global atmospheric chemistry model (EMAC). Acetaldehyde was  
624 found to have the highest discrepancy between the observations and model simulations, with the simulated values to be lower up  
625 to a factor of 10. By adding an oceanic source of acetaldehyde produced via light-driven photodegradation of CDOM in the  
626 seawater, the model estimation improved significantly, especially over the Red Sea North. With the oceanic source added, modelled  
627 acetaldehyde became slightly overestimated in clean regions, suggesting that the emission rate employed represents an upper limit.  
628 The results indicate that the ocean plays an important role in the atmospheric acetaldehyde budget, under both clean and polluted  
629 conditions. The underestimated acetaldehyde in the model is significant as it will influence the atmospheric budget of e.g. PAN.  
630 As shown in Figure 1, multiple sources and formation pathways need to be considered to better understand the atmospheric budget  
631 of acetaldehyde. Additional laboratory experiments and field measurements are necessary in order to verify all possible  
632 atmospheric formation mechanisms and to improve model simulations.

#### 633 **Data availability.**

634 Data will be made available via: <https://edmond.mpdl.mpg.de/imeji/>

#### 635 **Author contributions.**

636 AE and CS performed PTR-ToF-MS measurement and preliminary data processing. NW conducted data analysis and drafted the  
637 article. AP performed EMAC model simulation. EB and LE are responsible for NMHC measurements and data. DD, BH and HF  
638 provided formaldehyde data. Ozone and actinic flux data were contributed by JS and JNC. Methane and carbon monoxide data  
639 were provided by JP. JL designed and realized the campaign. JW supervised the study. All authors contributed to editing the draft  
640 and approved the submitted version.

#### 641 **Competing interest.**

642 The authors declare that they have no conflict of interest.

## 643 Acknowledgements

644 We acknowledge the collaboration with the King Abdullah University of Science and Technology (KAUST), the Kuwait Institute  
645 for Scientific Research (KISR) and the Cyprus Institute (CyI) to fulfill the campaign. We would like to thank Captain Pavel Kirzner  
646 and the crew for their full support on-board the Kommandor Iona, Hays Ships Ltd,. We are grateful for the support from all  
647 members involved in AQABA campaign, especially Dr. Hartwig Harder for his general organization onboard of the campaign;  
648 and Dr. Marcel Dorf, Claus Koeppel, Thomas Klüpfel and Rolf Hofmann for logistical organization and their help with preparation  
649 and setup. We would like to express our gratitude to Ivan Tadic and Philipp Eger for the use of ship exhaust contamination flag.  
650 Nijing Wang would acknowledges the European Union's Horizon 2020 research and innovation programme under the Marie  
651 Skłodowska-Curie grant agreement No. 674911.

## 652 References

- 653 Abdelhady, S., Borello, D., Shaban, A., and Rispoli, F.: Viability Study of Biomass Power Plant Fired with Rice Straw in Egypt,  
654 Energy Procedia, 61, 211-215, <https://doi.org/10.1016/j.egypro.2014.11.1072>, 2014.
- 655 Aklilu, Y.-a., Cho, S., Zhang, Q., and Taylor, E.: Source apportionment of volatile organic compounds measured near a cold heavy  
656 oil production area, Atmospheric Research, 206, 75-86, <https://doi.org/10.1016/j.atmosres.2018.02.007>, 2018.
- 657 Altshuller, A. P.: Production of aldehydes as primary emissions and from secondary atmospheric reactions of alkenes and alkanes  
658 during the night and early morning hours, Atmospheric Environment. Part A. General Topics, 27, 21-32,  
659 [https://doi.org/10.1016/0960-1686\(93\)90067-9](https://doi.org/10.1016/0960-1686(93)90067-9), 1993.
- 660 Apel, E. C., Brauers, T., Koppmann, R., Bandowe, B., Boßmeyer, J., Holzke, C., Tillmann, R., Wahner, A., Wegener, R., Brunner,  
661 A., Jocher, M., Ruuskanen, T., Spirig, C., Steigner, D., Steinbrecher, R., Gomez Alvarez, E., Müller, K., Burrows, J. P., Schade,  
662 G., Solomon, S. J., Ladstätter-Weissenmayer, A., Simmonds, P., Young, D., Hopkins, J. R., Lewis, A. C., Legreid, G., Reimann,  
663 S., Hansel, A., Wisthaler, A., Blake, R. S., Ellis, A. M., Monks, P. S., and Wyche, K. P.: Intercomparison of oxygenated volatile  
664 organic compound measurements at the SAPHIR atmosphere simulation chamber, Journal of Geophysical Research, 113,  
665 10.1029/2008jd009865, 2008.
- 666 Atkinson, R., Tuazon, E. C., and Aschmann, S. M.: Products of the Gas-Phase Reactions of a Series of 1-Alkenes and 1-  
667 Methylcyclohexene with the OH Radical in the Presence of NO, Environmental Science & Technology, 29, 1674-1680,  
668 10.1021/es00006a035, 1995.
- 669 Atkinson, R., and Arey, J.: Atmospheric Degradation of Volatile Organic Compounds, Chemical Reviews, 103, 4605-4638,  
670 10.1021/cr0206420, 2003.
- 671 Baboukas, E. D., Kanakidou, M., and Mihalopoulos, N.: Carboxylic acids in gas and particulate phase above the Atlantic Ocean,  
672 Journal of Geophysical Research: Atmospheres, 105, 14459-14471, 10.1029/1999jd900977, 2000.
- 673 Bates, T. S., Lamb, B. K., Guenther, A., Dignon, J., and Stoiber, R. E.: Sulfur emissions to the atmosphere from natural sources,  
674 Journal of Atmospheric Chemistry, 14, 315-337, 10.1007/bf00115242, 1992.
- 675 Beale, R., Dixon, J. L., Arnold, S. R., Liss, P. S., and Nightingale, P. D.: Methanol, acetaldehyde, and acetone in the surface waters  
676 of the Atlantic Ocean, Journal of Geophysical Research: Oceans, 118, 5412-5425, 10.1002/jgrc.20322, 2013.
- 677 Borbon, A., Gilman, J. B., Kuster, W. C., Grand, N., Chevaillier, S., Colomb, A., Dolgorouky, C., Gros, V., Lopez, M., Sarda-  
678 Esteve, R., Holloway, J., Stutz, J., Petetin, H., McKeen, S., Beekmann, M., Warneke, C., Parrish, D. D., and de Gouw, J. A.:  
679 Emission ratios of anthropogenic volatile organic compounds in northern mid-latitude megacities: Observations versus emission  
680 inventories in Los Angeles and Paris, Journal of Geophysical Research: Atmospheres, 118, 2041-2057, 10.1002/jgrd.50059, 2013.
- 681 Bourtsoukidis, E., Williams, J., Kesselmeier, J., Jacobi, S., and Bonn, B.: From emissions to ambient mixing ratios: online seasonal  
682 field measurements of volatile organic compounds over a Norway spruce-dominated forest in central Germany, Atmos. Chem.  
683 Phys., 14, 6495-6510, <https://doi.org/10.5194/acp-14-6495-2014>, 2014.
- 684 Bourtsoukidis, E., Ernle, L., Crowley, J. N., Lelieveld, J., Paris, J.-D., Pozzer, A., Walter, D., and Williams, J.: Non-methane  
685 hydrocarbon (C<sub>2</sub>-C<sub>8</sub>) sources and sinks around the Arabian Peninsula, Atmospheric Chemistry and Physics, 19, 7209-7232,  
686 10.5194/acp-19-7209-2019, 2019.
- 687 Bourtsoukidis, E., Pozzer, A., Sattler, T., Matthaios, V. N., Ernle, L., Edtbauer, A., Fischer, H., Konemann, T., Osipov, S., Paris,  
688 J. D., Pfannerstill, E. Y., Stonner, C., Tadic, I., Walter, D., Wang, N., Lelieveld, J., and Williams, J.: The Red Sea Deep Water is  
689 a potent source of atmospheric ethane and propane, Nat Commun, 11, 447, 10.1038/s41467-020-14375-0, 2020.



Boreddy, S. K. R., Kawamura, K., and Tachibana, E.: Long-term (2001–2013) observations of water-soluble dicarboxylic acids and related compounds over the western North Pacific: trends, seasonality and source apportionment, *Scientific Reports*, 7, 8518, 10.1038/s41598-017-08745-w, 2017.

Brilli, F., Gioli, B., Ciccioli, P., Zona, D., Loreto, F., Janssens, I. A., and Ceulemans, R.: Proton Transfer Reaction Time-of-Flight Mass Spectrometric (PTR-TOF-MS) determination of volatile organic compounds (VOCs) emitted from a biomass fire developed under stable nocturnal conditions, *Atmospheric Environment*, 97, 54-67, 10.1016/j.atmosenv.2014.08.007, 2014.

Buhr, K., van Ruth, S., and Delahunty, C.: Analysis of volatile flavour compounds by Proton Transfer Reaction-Mass Spectrometry: fragmentation patterns and discrimination between isobaric and isomeric compounds, *International Journal of Mass Spectrometry*, 221, 1-7, [https://doi.org/10.1016/S1387-3806\(02\)00896-5](https://doi.org/10.1016/S1387-3806(02)00896-5), 2002.

Cabrera-Perez, D., Taraborrelli, D., Sander, R., and Pozzer, A.: Global atmospheric budget of simple monocyclic aromatic compounds, *Atmospheric Chemistry and Physics*, 16, 6931-6947, 10.5194/acp-16-6931-2016, 2016.

Carrier, P., Hannachi, H., and Mouvier, G.: The chemistry of carbonyl compounds in the atmosphere—A review, *Atmospheric Environment* (1967), 20, 2079-2099, [https://doi.org/10.1016/0004-6981\(86\)90304-5](https://doi.org/10.1016/0004-6981(86)90304-5), 1986.

Celik, S., Drewnick, F., Fachinger, F., Brooks, J., Darbyshire, E., Coe, H., Paris, J. D., Eger, P. G., Schuladen, J., Tadic, I., Friedrich, N., Dienhart, D., Hottmann, B., Fischer, H., Crowley, J. N., Harder, H., and Borrmann, S.: Influence of vessel characteristics and atmospheric processes on the gas and particle phase of ship emission plumes: In-situ measurements in the Mediterranean Sea and around the Arabian Peninsula, *Atmos. Chem. Phys. Discuss.*, 2019, 1-36, 10.5194/acp-2019-859, 2019.

Ciuraru, R., Fine, L., van Pinxteren, M., D'Anna, B., Herrmann, H., and George, C.: Photosensitized production of functionalized and unsaturated organic compounds at the air-sea interface, *Sci Rep*, 5, 12741, 10.1038/srep12741, 2015.

Cochran, R. E., Laskina, O., Jayarathne, T., Laskin, A., Laskin, J., Lin, P., Sultana, C., Lee, C., Moore, K. A., Cappa, C. D., Bertram, T. H., Prather, K. A., Grassian, V. H., and Stone, E. A.: Analysis of Organic Anionic Surfactants in Fine and Coarse Fractions of Freshly Emitted Sea Spray Aerosol, *Environ Sci Technol*, 50, 2477-2486, 10.1021/acs.est.5b04053, 2016.

Colomb, A., Williams, J., Crowley, J., Gros, V., Hofmann, R., Salisbury, G., Klüpfel, T., Kormann, R., Stickler, A., Forster, C., and Lelieveld, J.: Airborne Measurements of Trace Organic Species in the Upper Troposphere Over Europe: the Impact of Deep Convection, *Environmental Chemistry*, 3, 244, 10.1071/en06020, 2006.

Colomb, A., Gros, V., Alvain, S., Sarda-Esteve, R., Bonsang, B., Moulin, C., Klüpfel, T., and Williams, J.: Variation of atmospheric volatile organic compounds over the Southern Indian Ocean (30 - 49°S), *Environmental Chemistry*, 6, 70, 10.1071/en08072, 2009.

de Gouw, J., and Warneke, C.: Measurements of volatile organic compounds in the earth's atmosphere using proton-transfer-reaction mass spectrometry, *Mass Spectrometry Reviews*, 26, 223-257, 2007.

de Gouw, J. A., Middlebrook, A. M., Warneke, C., Goldan, P. D., Kuster, W. C., Roberts, J. M., Fehsenfeld, F. C., Worsnop, D. R., Canagaratna, M. R., Pszenny, A. A. P., Keene, W. C., Marchewka, M., Bertman, S. B., and Bates, T. S.: Budget of organic carbon in a polluted atmosphere: Results from the New England Air Quality Study in 2002, *Journal of Geophysical Research: Atmospheres*, 110, doi:10.1029/2004JD005623, 2005.

Dixon, J. L., Beale, R., and Nightingale, P. D.: Production of methanol, acetaldehyde, and acetone in the Atlantic Ocean, *Geophysical Research Letters*, 40, 4700-4705, 10.1002/grl.50922, 2013.

Dolgorouky, C., Gros, V., Sarda-Esteve, R., Sinha, V., Williams, J., Marchand, N., Sauvage, S., Poulain, L., Sciare, J., and Bonsang, B.: Total OH reactivity measurements in Paris during the 2010 MEGAPOLI winter campaign, *Atmospheric Chemistry and Physics*, 12, 9593-9612, 10.5194/acp-12-9593-2012, 2012.

Dong, D., Shao, M., Li, Y., Lu, S., Wang, Y., Ji, Z., and Tang, D.: Carbonyl emissions from heavy-duty diesel vehicle exhaust in China and the contribution to ozone formation potential, *Journal of Environmental Sciences*, 26, 122-128, [https://doi.org/10.1016/S1001-0742\(13\)60387-3](https://doi.org/10.1016/S1001-0742(13)60387-3), 2014.

Edtbauer, A., Stönnner, C., Pfannerstill, E. Y., Berasategui, M., Walter, D., Crowley, J. N., Lelieveld, J., and Williams, J.: A new marine biogenic emission: methane sulfonamide (MSAM), dimethyl sulfide (DMS), and dimethyl sulfone (DMSO<sub>2</sub>) measured in air over the Arabian Sea, *Atmospheric Chemistry and Physics*, 20, 6081-6094, 10.5194/acp-20-6081-2020, 2020.

Edwards, P. M., Brown, S. S., Roberts, J. M., Ahmadov, R., Banta, R. M., deGouw, J. A., Dube, W. P., Field, R. A., Flynn, J. H., Gilman, J. B., Graus, M., Helmig, D., Koss, A., Langford, A. O., Lefer, B. L., Lerner, B. M., Li, R., Li, S. M., McKeen, S. A., Murphy, S. M., Parrish, D. D., Senff, C. J., Soltis, J., Stutz, J., Sweeney, C., Thompson, C. R., Trainer, M. K., Tsai, C., Veres, P. R., Washenfelder, R. A., Warneke, C., Wild, R. J., Young, C. J., Yuan, B., and Zamora, R.: High winter ozone pollution from carbonyl photolysis in an oil and gas basin, *Nature*, 514, 351-354, 10.1038/nature13767, 2014.

740 Eger, P. G., Friedrich, N., Schuladen, J., Shenolikar, J., Fischer, H., Tadic, I., Harder, H., Martinez, M., Rohloff, R., Tauer, S.,  
741 Drewnick, F., Fachinger, F., Brooks, J., Darbyshire, E., Sciare, J., Pikridas, M., Lelieveld, J., and Crowley, J. N.: Shipborne  
742 measurements of ClNO<sub>2</sub> in the Mediterranean Sea and around the Arabian Peninsula during summer, *Atmospheric Chemistry and*  
743 *Physics*, 19, 12121-12140, 10.5194/acp-19-12121-2019, 2019a.

744 Eger, P. G., Schuladen, J., Sobanski, N., Fischer, H., Karu, E., Williams, J., Riva, M., Zha, Q., Ehn, M., Quéléver, L. L. J.,  
745 Schallhart, S., Lelieveld, J., and Crowley, J. N.: Pyruvic acid in the boreal forest: first measurements and impact on radical  
746 chemistry, *Atmos. Chem. Phys. Discuss.*, 2019, 1-24, 10.5194/acp-2019-768, 2019b.

747 Ellis, A. M., and Mayhew, C. A.: *Proton transfer reaction mass spectrometry: principles and applications*, John Wiley & Sons,  
748 2013.

749 Erickson, M. H., Gueneron, M., and Jobson, B. T.: Measuring long chain alkanes in diesel engine exhaust by thermal desorption  
750 PTR-MS, *Atmospheric Measurement Techniques*, 7, 225-239, 10.5194/amt-7-225-2014, 2014.

751 Fall, R.: Abundant Oxygenates in the Atmosphere: A Biochemical Perspective, *Chemical Reviews*, 103, 4941-4952,  
752 10.1021/cr0206521, 2003.

753 Fan, J., and Zhang, R.: Atmospheric Oxidation Mechanism of Isoprene, *Environmental Chemistry*, 1, 140-149,  
754 <https://doi.org/10.1071/EN04045>, 2004.

755 Finlayson-Pitts, B. J., and Pitts, J. N.: Tropospheric Air Pollution: Ozone, Airborne Toxics, Polycyclic Aromatic Hydrocarbons,  
756 and Particles, *Science*, 276, 1045, 10.1126/science.276.5315.1045, 1997.

757 Finlayson-Pitts, B. J., and Pitts Jr, J. N.: *Chemistry of the upper and lower atmosphere: theory, experiments, and applications*,  
758 Elsevier, 1999.

759 Fischer, E. V., Jacob, D. J., Millet, D. B., Yantosca, R. M., and Mao, J.: The role of the ocean in the global atmospheric budget of  
760 acetone, *Geophysical Research Letters*, 39, n/a-n/a, 10.1029/2011gl050086, 2012.

761 Fischer, H., Pozzer, A., Schmitt, T., Jöckel, P., Klippel, T., Taraborrelli, D., and Lelieveld, J.: Hydrogen peroxide in the marine  
762 boundary layer over the South Atlantic during the OOMPH cruise in March 2007, *Atmospheric Chemistry and Physics*, 15, 6971-  
763 6980, 10.5194/acp-15-6971-2015, 2015.

764 Gantt, B., Meskhidze, N., Facchini, M. C., Rinaldi, M., Ceburnis, D., and Dowd, C. D.: Wind speed dependent size-  
765 resolved parameterization for the organic mass fraction of sea spray aerosol, *Atmospheric Chemistry and Physics*, 11, 8777-8790,  
766 10.5194/acp-11-8777-2011, 2011.

767 Gentner, D. R., Isaacman, G., Worton, D. R., Chan, A. W. H., Dallmann, T. R., Davis, L., Liu, S., Day, D. A., Russell, L. M.,  
768 Wilson, K. R., Weber, R., Guha, A., Harley, R. A., and Goldstein, A. H.: Elucidating secondary organic aerosol from diesel and  
769 gasoline vehicles through detailed characterization of organic carbon emissions, *Proceedings of the National Academy of Sciences*,  
770 109, 18318, 10.1073/pnas.1212272109, 2012.

771 Gilman, J. B., Lerner, B. M., Kuster, W. C., and de Gouw, J. A.: Source signature of volatile organic compounds from oil and  
772 natural gas operations in northeastern Colorado, *Environ Sci Technol*, 47, 1297-1305, 10.1021/es304119a, 2013.

773 Griffith, E. C., Carpenter, B. K., Shoemaker, R. K., and Vaida, V.: Photochemistry of aqueous pyruvic acid, *Proceedings of the*  
774 *National Academy of Sciences*, 110, 11714, 10.1073/pnas.1303206110, 2013.

775 Gueneron, M., Erickson, M. H., VanderSchelden, G. S., and Jobson, B. T.: PTR-MS fragmentation patterns of gasoline  
776 hydrocarbons, *International Journal of Mass Spectrometry*, 379, 97-109, 10.1016/j.ijms.2015.01.001, 2015.

777 Guo, H., Ling, Z. H., Cheung, K., Wang, D. W., Simpson, I. J., and Blake, D. R.: Acetone in the atmosphere of Hong Kong:  
778 Abundance, sources and photochemical precursors, *Atmospheric Environment*, 65, 80-88, 10.1016/j.atmosenv.2012.10.027, 2013.

779 Holzinger, R., Warneke, C., Hansel, A., Jordan, A., Lindinger, W., Scharffe, D. H., Schade, G., and Crutzen, P. J.: Biomass burning  
780 as a source of formaldehyde, acetaldehyde, methanol, acetone, acetonitrile, and hydrogen cyanide, *Geophysical Research Letters*,  
781 26, 1161-1164, 10.1029/1999gl900156, 1999.

782 Holzinger, R., Jordan, A., Hansel, A., and Lindinger, W.: Automobile Emissions of Acetonitrile: Assessment of its Contribution  
783 to the Global Source, *Journal of Atmospheric Chemistry*, 38, 187-193, 10.1023/A:1006435723375, 2001.

784 Holzinger, R., Williams, J., Salisbury, G., Klüpfel, T., de Reus, M., Traub, M., Crutzen, P. J., and Lelieveld, J.: Oxygenated  
785 compounds in aged biomass burning plumes over the Eastern Mediterranean: evidence for strong secondary production of methanol  
786 and acetone, *Atmos. Chem. Phys.*, 5, 39-46, 10.5194/acp-5-39-2005, 2005.

787 Hornbrook, R. S., Hills, A. J., Riemer, D. D., Abdelhamid, A., Flocke, F. M., Hall, S. R., Huey, L. G., Knapp, D. J., Liao, J.,  
788 Mauldin III, R. L., Montzka, D. D., Orlando, J. J., Shepson, P. B., Sive, B., Staebler, R. M., Tanner, D. J., Thompson, C. R.,

Turnipseed, A., Ullmann, K., Weinheimer, A. J., and Apel, E. C.: Arctic springtime observations of volatile organic compounds during the OASIS-2009 campaign, *Journal of Geophysical Research: Atmospheres*, 121, 9789-9813, 10.1002/2015jd024360, 2016.

Huang, C., Hu, Q., Wang, H., Qiao, L., Jing, S., Wang, H., Zhou, M., Zhu, S., Ma, Y., Lou, S., Li, L., Tao, S., Li, Y., and Lou, D.: Emission factors of particulate and gaseous compounds from a large cargo vessel operated under real-world conditions, *Environ Pollut*, 242, 667-674, 10.1016/j.envpol.2018.07.036, 2018.

IUPAC Task Group on Atmospheric Chemical Kinetic Data Evaluation, (<http://iupac.pole-ether.fr>).

Jacob, D. J., Field, B. D., Jin, E. M., Bey, I., Li, Q., Logan, J. A., Yantosca, R. M., and Singh, H. B.: Atmospheric budget of acetone, *Journal of Geophysical Research: Atmospheres*, 107, ACH 5-1-ACH 5-17, 10.1029/2001jd000694, 2002.

Jardine, K. J., Sommer, E. D., Saleska, S. R., Huxman, T. E., Harley, P. C., and Abrell, L.: Gas Phase Measurements of Pyruvic Acid and Its Volatile Metabolites, *Environmental Science & Technology*, 44, 2454-2460, 10.1021/es903544p, 2010.

Ji, Y., Zhao, J., Terazono, H., Misawa, K., Levitt, N. P., Li, Y., Lin, Y., Peng, J., Wang, Y., Duan, L., Pan, B., Zhang, F., Feng, X., An, T., Marrero-Ortiz, W., Secrest, J., Zhang, A. L., Shibuya, K., Molina, M. J., and Zhang, R.: Reassessing the atmospheric oxidation mechanism of toluene, *Proceedings of the National Academy of Sciences*, 114, 8169, 10.1073/pnas.1705463114, 2017.

Jöckel, P., Kerkweg, A., Pozzer, A., Sander, R., Tost, H., Riede, H., Baumgaertner, A., Gromov, S., and Kern, B.: Development cycle 2 of the Modular Earth Submodel System (MESSy2), *Geoscientific Model Development*, 3, 717-752, 10.5194/gmd-3-717-2010, 2010.

Khan, M. A. H., Cooke, M. C., Utembe, S. R., Archibald, A. T., Maxwell, P., Morris, W. C., Xiao, P., Derwent, R. G., Jenkin, M. E., Percival, C. J., Walsh, R. C., Young, T. D. S., Simmonds, P. G., Nickless, G., O'Doherty, S., and Shallcross, D. E.: A study of global atmospheric budget and distribution of acetone using global atmospheric model STOCHEM-CRI, *Atmospheric Environment*, 112, 269-277, 10.1016/j.atmosenv.2015.04.056, 2015.

Kieber, D. J., and Mopper, K.: Photochemical formation of glyoxylic and pyruvic acids in seawater, *Marine Chemistry*, 21, 135-149, [https://doi.org/10.1016/0304-4203\(87\)90034-X](https://doi.org/10.1016/0304-4203(87)90034-X), 1987.

Kieber, R. J., Zhou, X., and Mopper, K.: Formation of carbonyl compounds from UV-induced photodegradation of humic substances in natural waters: Fate of riverine carbon in the sea, *Limnology and Oceanography*, 35, 1503-1515, 10.4319/lo.1990.35.7.1503, 1990.

Kim, K.-H., Hong, Y.-J., Pal, R., Jeon, E.-C., Koo, Y.-S., and Sunwoo, Y.: Investigation of carbonyl compounds in air from various industrial emission sources, *Chemosphere*, 70, 807-820, <https://doi.org/10.1016/j.chemosphere.2007.07.025>, 2008.

Koss, A., Yuan, B., Warneke, C., Gilman, J. B., Lerner, B. M., Veres, P. R., Peischl, J., Eilerman, S., Wild, R., Brown, S. S., Thompson, C. R., Ryerson, T., Hanisco, T., Wolfe, G. M., Clair, J. M. S., Thayer, M., Keutsch, F. N., Murphy, S., and de Gouw, J.: Observations of VOC emissions and photochemical products over US oil- and gas-producing regions using high-resolution H3O+ CIMS (PTR-ToF-MS), *Atmos. Meas. Tech.*, 10, 2941-2968, 10.5194/amt-10-2941-2017, 2017.

Koss, A. R., de Gouw, J., Warneke, C., Gilman, J. B., Lerner, B. M., Graus, M., Yuan, B., Edwards, P., Brown, S. S., Wild, R., Roberts, J. M., Bates, T. S., and Quinn, P. K.: Photochemical aging of volatile organic compounds associated with oil and natural gas extraction in the Uintah Basin, UT, during a wintertime ozone formation event, *Atmospheric Chemistry and Physics*, 15, 5727-5741, 10.5194/acp-15-5727-2015, 2015.

Koss, A. R., Sekimoto, K., Gilman, J. B., Selimovic, V., Coggon, M. M., Zarzana, K. J., Yuan, B., Lerner, B. M., Brown, S. S., Jimenez, J. L., Krechmer, J., Roberts, J. M., Warneke, C., Yokelson, R. J., and de Gouw, J.: Non-methane organic gas emissions from biomass burning: identification, quantification, and emission factors from PTR-ToF during the FIREX 2016 laboratory experiment, *Atmospheric Chemistry and Physics*, 18, 3299-3319, 10.5194/acp-18-3299-2018, 2018.

Kroll, J. H., Ng, N. L., Murphy, S. M., Varutbangkul, V., Flagan, R. C., and Seinfeld, J. H.: Chamber studies of secondary organic aerosol growth by reactive uptake of simple carbonyl compounds, *Journal of Geophysical Research*, 110, 10.1029/2005jd006004, 2005.

Lelieveld, J., Gromov, S., Pozzer, A., and Taraborrelli, D.: Global tropospheric hydroxyl distribution, budget and reactivity, *Atmospheric Chemistry and Physics*, 16, 12477-12493, 10.5194/acp-16-12477-2016, 2016.

Lewis, A., Hopkins, J., Carpenter, L., Stanton, J., Read, K., and Pilling, M.: Sources and sinks of acetone, methanol, and acetaldehyde in North Atlantic marine air, *Atmospheric Chemistry and Physics*, 5, 1963-1974, 2005.

Li, S.-M., Leithead, A., Moussa, S. G., Liggio, J., Moran, M. D., Wang, D., Hayden, K., Darlington, A., Gordon, M., Staebler, R., Makar, P. A., Stroud, C. A., McLaren, R., Liu, P. S. K., O'Brien, J., Mittermeier, R. L., Zhang, J., Marson, G., Cober, S. G., Wolde, M., and Wentzell, J. J. B.: Differences between measured and reported volatile organic compound emissions from oil sands facilities in Alberta, Canada, *Proceedings of the National Academy of Sciences*, 114, E3756, 10.1073/pnas.1617862114, 2017.

839 Lindinger, W., Hansel, A., and Jordan, A.: On-line monitoring of volatile organic compounds at pptv levels by means of proton-  
840 transfer-reaction mass spectrometry (PTR-MS) medical applications, food control and environmental research, *International*  
841 *Journal of Mass Spectrometry and Ion Processes*, 173, 191-241, 1998.

842 Lobert, J. M., Scharffe, D. H., Hao, W. M., and Crutzen, P. J.: Importance of biomass burning in the atmospheric budgets of  
843 nitrogen-containing gases, *Nature*, 346, 552-554, 10.1038/346552a0, 1990.

844 Marandino, C. A., De Bruyn, W. J., Miller, S. D., Prather, M. J., and Saltzman, E. S.: Oceanic uptake and the global atmospheric  
845 acetone budget, *Geophysical Research Letters*, 32, 10.1029/2005GL023285, 2005.

846 Millet, D. B., Guenther, A., Siegel, D. A., Nelson, N. B., Singh, H. B., de Gouw, J. A., Warneke, C., Williams, J., Eerdekens, G.,  
847 and Sinha, V.: Global atmospheric budget of acetaldehyde: 3-D model analysis and constraints from in-situ and satellite  
848 observations, *Atmospheric Chemistry and Physics*, 10, 3405-3425, 2010.

849 Mochida, M., Kitamori, Y., Kawamura, K., Nojiri, Y., and Suzuki, K.: Fatty acids in the marine atmosphere: Factors governing  
850 their concentrations and evaluation of organic films on sea-salt particles, *Journal of Geophysical Research: Atmospheres*, 107,  
851 AAC 1-1-AAC 1-10, 10.1029/2001jd001278, 2002.

852 Müller, M., Graus, M., Wisthaler, A., Hansel, A., Metzger, A., Dommen, J., and Baltensperger, U.: Analysis of high mass resolution  
853 PTR-TOF mass spectra from 1,3,5-trimethylbenzene (TMB) environmental chamber experiments, *Atmospheric Chemistry and*  
854 *Physics*, 12, 829-843, 10.5194/acp-12-829-2012, 2012.

855 Müller, M., Mikoviny, T., Jud, W., D'Anna, B., and Wisthaler, A.: A new software tool for the analysis of high resolution PTR-  
856 TOF mass spectra, *Chemometrics and Intelligent Laboratory Systems*, 127, 158-165, 10.1016/j.chemolab.2013.06.011, 2013.

857 Meusel, H., Kuhn, U., Reiffs, A., Mallik, C., Harder, H., Martinez, M., Schuladen, J., Bohn, B., Parchatka, U., and Crowley, J. N.:  
858 Daytime formation of nitrous acid at a coastal remote site in Cyprus indicating a common ground source of atmospheric HONO  
859 and NO, *Atmospheric Chemistry and Physics*, 16, 14475-14493, 2016.

860 Nogueira, T., Dominutti, P. A., de Carvalho, L. R. F., Fornaro, A., and Andrade, M. d. F.: Formaldehyde and acetaldehyde  
861 measurements in urban atmosphere impacted by the use of ethanol biofuel: Metropolitan Area of Sao Paulo (MASP), 2012–2013,  
862 *Fuel*, 134, 505-513, 10.1016/j.fuel.2014.05.091, 2014.

863 Northway, M. J., de Gouw, J. A., Fahey, D. W., Gao, R. S., Warneke, C., Roberts, J. M., and Flocke, F.: Evaluation of the role of  
864 heterogeneous oxidation of alkenes in the detection of atmospheric acetaldehyde, *Atmospheric Environment*, 38, 6017-6028,  
865 10.1016/j.atmosenv.2004.06.039, 2004.

866 Pfannerstill, E. Y., Wang, N., Edtbauer, A., Bourtsoukidis, E., Crowley, J. N., Dienhart, D., Eger, P. G., Ernle, L., Fischer, H.,  
867 Hottmann, B., Paris, J.-D., Stöner, C., Tadic, I., Walter, D., Lelieveld, J., and Williams, J.: Shipborne measurements of total OH  
868 reactivity around the Arabian Peninsula and its role in ozone chemistry, *Atmospheric Chemistry and Physics*, 19, 11501-11523,  
869 10.5194/acp-19-11501-2019, 2019.

870 Pozzer, A., Jöckel, P., Tost, H., Sander, R., Ganzeveld, L., Kerkweg, A., and Lelieveld, J.: Simulating organic species with the  
871 global atmospheric chemistry general circulation model ECHAM5/MESSy1: a comparison of model results with observations,  
872 *Atmos. Chem. Phys.*, 7, 2527-2550, 10.5194/acp-7-2527-2007, 2007.

873 Pozzer, A., de Meij, A., Pringle, K. J., Tost, H., Doering, U. M., van Aardenne, J., and Lelieveld, J.: Distributions and regional  
874 budgets of aerosols and their precursors simulated with the EMAC chemistry-climate model, *Atmospheric Chemistry and Physics*,  
875 12, 961-987, 10.5194/acp-12-961-2012, 2012.

876 Read, K. A., Carpenter, L. J., Arnold, S. R., Beale, R., Nightingale, P. D., Hopkins, J. R., Lewis, A. C., Lee, J. D., Mendes, L., and  
877 Pickering, S. J.: Multiannual observations of acetone, methanol, and acetaldehyde in remote tropical atlantic air: implications for  
878 atmospheric OVOC budgets and oxidative capacity, *Environ Sci Technol*, 46, 11028-11039, 10.1021/es302082p, 2012.

879 Reda, A. A., Schnelle-Kreis, J., Orasche, J., Abbaszade, G., Lintelmann, J., Arteaga-Salas, J. M., Stengel, B., Rabe, R., Harndorf,  
880 H., Sippula, O., Streibel, T., and Zimmermann, R.: Gas phase carbonyl compounds in ship emissions: Differences between diesel  
881 fuel and heavy fuel oil operation, *Atmospheric Environment*, 94, 467-478, 10.1016/j.atmosenv.2014.05.053, 2014.

882 Reed Harris, A. E., Ervens, B., Shoemaker, R. K., Kroll, J. A., Rapf, R. J., Griffith, E. C., Monod, A., and Vaida, V.: Photochemical  
883 kinetics of pyruvic acid in aqueous solution, *J Phys Chem A*, 118, 8505-8516, 10.1021/jp502186q, 2014.

884 Reed Harris, A. E., Doussin, J.-F., Carpenter, B. K., and Vaida, V.: Gas-Phase Photolysis of Pyruvic Acid: The Effect of Pressure  
885 on Reaction Rates and Products, *The Journal of Physical Chemistry A*, 120, 10123-10133, 10.1021/acs.jpca.6b09058, 2016.

886 Roberts, J. M., Fehsenfeld, F. C., Liu, S. C., Bollinger, M. J., Hahn, C., Albritton, D. L., and Sievers, R. E.: Measurements of  
887 aromatic hydrocarbon ratios and NO<sub>x</sub> concentrations in the rural troposphere: Observation of air mass photochemical aging and  
888 NO<sub>x</sub> removal, *Atmospheric Environment* (1967), 18, 2421-2432, [https://doi.org/10.1016/0004-6981\(84\)90012-X](https://doi.org/10.1016/0004-6981(84)90012-X), 1984.

889 Roeckner, E., Brokopf, R., Esch, M., Giorgetta, M., Hagemann, S., Kornblueh, L., Manzini, E., Schlese, U., and Schulzweida, U.:  
890 Sensitivity of Simulated Climate to Horizontal and Vertical Resolution in the ECHAM5 Atmosphere Model, *Journal of Climate*,  
891 19, 3771-3791, 10.1175/JCLI3824.1, 2006.

892 Rutter, A. P., Griffin, R. J., Cevik, B. K., Shakya, K. M., Gong, L., Kim, S., Flynn, J. H., and Lefer, B. L.: Sources of air pollution  
893 in a region of oil and gas exploration downwind of a large city, *Atmospheric Environment*, 120, 89-99,  
894 10.1016/j.atmosenv.2015.08.073, 2015.

895 Sahu, L. K., Tripathi, N., and Yadav, R.: Contribution of biogenic and photochemical sources to ambient VOCs during winter to  
896 summer transition at a semi-arid urban site in India, *Environ Pollut*, 229, 595-606, 10.1016/j.envpol.2017.06.091, 2017.

897 Said, N., El-Shatoury, S. A., Díaz, L. F., and Zamorano, M.: Quantitative appraisal of biomass resources and their energy potential  
898 in Egypt, *Renewable and Sustainable Energy Reviews*, 24, 84-91, <https://doi.org/10.1016/j.rser.2013.03.014>, 2013.

899 Sander, R.: Compilation of Henry's law constants (version 4.0) for water as solvent, *Atmospheric Chemistry and Physics*, 15, 4399-  
900 4981, 10.5194/acp-15-4399-2015, 2015.

901 Sander, R., Baumgaertner, A., Cabrera-Perez, D., Frank, F., Gromov, S., Grooß, J.-U., Harder, H., Huijnen, V., Jöckel, P., Karydis,  
902 V. A., Niemeyer, K. E., Pozzer, A., Riede, H., Schultz, M. G., Taraborrelli, D., and Tauer, S.: The community atmospheric  
903 chemistry box model CAABA/MECCA-4.0, *Geoscientific Model Development*, 12, 1365-1385, 10.5194/gmd-12-1365-2019,  
904 2019.

905 Schauer, J. J., Kleeman, M. J., Cass, G. R., and Simoneit, B. R. T.: Measurement of Emissions from Air Pollution Sources. 3.  
906 C1-C29 Organic Compounds from Fireplace Combustion of Wood, *Environmental Science & Technology*, 35, 1716-1728,  
907 10.1021/es001331e, 2001.

908 Schlundt, C., Tegtmeier, S., Lennartz, S. T., Bracher, A., Cheah, W., Krüger, K., Quack, B., and Marandino, C. A.: Oxygenated  
909 volatile organic carbon in the western Pacific convective center: ocean cycling, air-sea gas exchange and atmospheric transport,  
910 *Atmospheric Chemistry and Physics*, 17, 10837-10854, 10.5194/acp-17-10837-2017, 2017.

911 Sheng, J., Zhao, D., Ding, D., Li, X., Huang, M., Gao, Y., Quan, J., and Zhang, Q.: Characterizing the level, photochemical  
912 reactivity, emission, and source contribution of the volatile organic compounds based on PTR-TOF-MS during winter haze period  
913 in Beijing, China, *Atmospheric Research*, 212, 54-63, <https://doi.org/10.1016/j.atmosres.2018.05.005>, 2018.

914 Simpson, I. J., Blake, N. J., Barletta, B., Diskin, G. S., Fuelberg, H. E., Gorham, K., Huey, L. G., Meinardi, S., Rowland, F. S.,  
915 Vay, S. A., Weinheimer, A. J., Yang, M., and Blake, D. R.: Characterization of trace gases measured over Alberta oil sands mining  
916 operations: 76 speciated C<sub>2</sub>-C<sub>10</sub> volatile organic compounds (VOCs), CO<sub>2</sub>, CH<sub>4</sub>, CO, NO, NO<sub>2</sub>, NO<sub>y</sub>, O<sub>3</sub> and SO<sub>2</sub>, *Atmos. Chem.*  
917 *Phys.*, 10, 11931-11954, 10.5194/acp-10-11931-2010, 2010.

918 Singh, H. B., O'hara, D., Herlth, D., Sachse, W., Blake, D., Bradshaw, J., Kanakidou, M., and Crutzen, P.: Acetone in the  
919 atmosphere: Distribution, sources, and sinks, *Journal of Geophysical Research: Atmospheres*, 99, 1805-1819, 1994.

920 Singh, H. B., Tabazadeh, A., Evans, M. J., Field, B. D., Jacob, D. J., Sachse, G., Crawford, J. H., Shetter, R., and Brune, W. H.:  
921 Oxygenated volatile organic chemicals in the oceans: Inferences and implications based on atmospheric observations and air-sea  
922 exchange models, *Geophysical Research Letters*, 30, 10.1029/2003gl017933, 2003.

923 Singh, H. B.: Analysis of the atmospheric distribution, sources, and sinks of oxygenated volatile organic chemicals based on  
924 measurements over the Pacific during TRACE-P, *Journal of Geophysical Research*, 109, 10.1029/2003jd003883, 2004.

925 Sinha, V., Williams, J., Meyerhöfer, M., Riebesell, U., Paulino, A. I., and Larsen, A.: Air-sea fluxes of methanol, acetone,  
926 acetaldehyde, isoprene and DMS from a Norwegian fjord following a phytoplankton bloom in a mesocosm experiment, *Atmos.*  
927 *Chem. Phys.*, 7, 739-755, 10.5194/acp-7-739-2007, 2007.

928 Sjøstedt, S. J., Leaitch, W. R., Levasseur, M., Scarratt, M., Michaud, S., Motard-Côté, J., Burkhart, J. H., and Abbatt, J. P. D.:  
929 Evidence for the uptake of atmospheric acetone and methanol by the Arctic Ocean during late summer DMS-Emission plumes,  
930 *Journal of Geophysical Research: Atmospheres*, 117, n/a-n/a, 10.1029/2011jd017086, 2012.

931 Spanel, P., Doren, J., and Smith, D.: A selected ion flow tube study of the reactions of H<sub>3</sub>O<sup>+</sup>, NO<sup>+</sup>, and O<sub>2</sub><sup>+</sup> with saturated and  
932 unsaturated aldehydes and subsequent hydration of the product ions, *International Journal of Mass Spectrometry*, 213, 163-176,  
933 10.1016/S1387-3806(01)00531-0, 2002.

934 Steinberg, S. M., and Bada, J. L.: Oxalic, glyoxalic and pyruvic acids in eastern Pacific Ocean waters, *Journal of Marine Research*,  
935 42, 697-708, 10.1357/002224084788506068, 1984.

936 Stickler, A., Fischer, H., Williams, J., de Reus, M., Sander, R., Lawrence, M. G., Crowley, J. N., and Lelieveld, J.: Influence of  
937 summertime deep convection on formaldehyde in the middle and upper troposphere over Europe, *Journal of Geophysical Research*,  
938 111, 10.1029/2005jd007001, 2006.

939 Swarthout, R. F., Russo, R. S., Zhou, Y., Miller, B. M., Mitchell, B., Horsman, E., Lipsky, E., McCabe, D. C., Baum, E., and Sive,  
940 B. C.: Impact of Marcellus Shale natural gas development in southwest Pennsylvania on volatile organic compound emissions and  
941 regional air quality, *Environ Sci Technol*, 49, 3175-3184, 10.1021/es504315f, 2015.

942 Tadic, I., Crowley, J. N., Dienhart, D., Eger, P., Harder, H., Hottmann, B., Martinez, M., Parchatka, U., Paris, J.-D., Pozzer, A.,  
943 Rohloff, R., Schuladen, J., Shenolikar, J., Tauer, S., Lelieveld, J., and Fischer, H.: Net ozone production and its relationship to  
944 nitrogen oxides and volatile organic compounds in the marine boundary layer around the Arabian Peninsula, *Atmospheric*  
945 *Chemistry and Physics*, 20, 6769-6787, 10.5194/acp-20-6769-2020, 2020.

946 Tanimoto, H., Kameyama, S., Iwata, T., Inomata, S., and Omori, Y.: Measurement of air-sea exchange of dimethyl sulfide and  
947 acetone by PTR-MS coupled with gradient flux technique, *Environ Sci Technol*, 48, 526-533, 10.1021/es4032562, 2014.

948 Vaught, C.: Locating and estimating air emissions from sources of formaldehyde (revised), Midwest Research Inst., Cary, NC  
949 (United States), 1991.

950 United States Central Intelligence Agency: Middle East oil and gas, Washington, D.C.: Central Intelligence Agency, available at:  
951 <https://www.loc.gov/item/2007631392/> (last access: 26 November 2019), 2007.

952 Utah Division of Air Quality: Final Report: Uinta Basin Winter Ozone Study, 2014.

953 Wang, S., Hornbrook, R. S., Hills, A., Emmons, L. K., Tilmes, S., Lamarque, J. F., Jimenez, J. L., Campuzano-Jost, P., Nault, B.  
954 A., Crounse, J. D., Wennberg, P. O., Kim, M., Allen, H., Ryerson, T. B., Thompson, C. R., Peischl, J., Moore, F., Nance, D., Hall,  
955 B., Elkins, J., Tanner, D., Huey, L. G., Hall, S. R., Ullmann, K., Orlando, J. J., Tyndall, G. S., Flocke, F. M., Ray, E., Hanisco, T.  
956 F., Wolfe, G. M., St. Clair, J., Commane, R., Daube, B., Barletta, B., Blake, D. R., Weinzierl, B., Dollner, M., Conley, A., Vitt, F.,  
957 Wofsy, S. C., Riemer, D. D., and Apel, E. C.: Atmospheric Acetaldehyde: Importance of Air-Sea Exchange and a Missing Source  
958 in the Remote Troposphere, *Geophysical Research Letters*, 10.1029/2019gl082034, 2019.

959 Warneke, C., Karl, T., Judmaier, H., Hansel, A., Jordan, A., Lindinger, W., and Crutzen, P. J.: Acetone, methanol, and other  
960 partially oxidized volatile organic emissions from dead plant matter by abiological processes: Significance for atmospheric HOx  
961 chemistry, *Global Biogeochemical Cycles*, 13, 9-17, 10.1029/98GB02428, 1999.

962 Warneke, C., and de Gouw, J. A.: Organic trace gas composition of the marine boundary layer over the northwest Indian Ocean in  
963 April 2000, *Atmospheric Environment*, 35, 5923-5933, [https://doi.org/10.1016/S1352-2310\(01\)00384-3](https://doi.org/10.1016/S1352-2310(01)00384-3), 2001.

964 Warneke, C., Geiger, F., Edwards, P. M., Dube, W., Pétron, G., Kofler, J., Zahn, A., Brown, S. S., Graus, M., Gilman, J. B., Lerner,  
965 B. M., Peischl, J., Ryerson, T. B., de Gouw, J. A., and Roberts, J. M.: Volatile organic compound emissions from the oil and  
966 natural gas industry in the Uintah Basin, Utah: oil and gas well pad emissions compared to ambient air composition, *Atmospheric*  
967 *Chemistry and Physics*, 14, 10977-10988, 10.5194/acp-14-10977-2014, 2014.

968 Wennberg, P. O., Bates, K. H., Crounse, J. D., Dodson, L. G., McVay, R. C., Mertens, L. A., Nguyen, T. B., Praske, E., Schwantes,  
969 R. H., Smarte, M. D., St Clair, J. M., Teng, A. P., Zhang, X., and Seinfeld, J. H.: Gas-Phase Reactions of Isoprene and Its Major  
970 Oxidation Products, *Chemical Reviews*, 118, 3337-3390, 10.1021/acs.chemrev.7b00439, 2018.

971 Williams, J., Roberts, J. M., Bertman, S. B., Stroud, C. A., Fehsenfeld, F. C., Baumann, K., Buhr, M. P., Knapp, K., Murphy, P.  
972 C., Nowick, M., and Williams, E. J.: A method for the airborne measurement of PAN, PPN, and MPAN, *Journal of Geophysical*  
973 *Research: Atmospheres*, 105, 28943-28960, 10.1029/2000JD900373, 2000.

974 Williams, J., Pöschl, U., Crutzen, P. J., Hansel, A., Holzinger, R., Warneke, C., Lindinger, W., and Lelieveld, J.: An Atmospheric  
975 Chemistry Interpretation of Mass Scans Obtained from a Proton Transfer Mass Spectrometer Flown over the Tropical Rainforest  
976 of Surinam, *Journal of Atmospheric Chemistry*, 38, 133-166, 10.1023/A:1006322701523, 2001.

977 Williams, J., Holzinger, R., Gros, V., Xu, X., Atlas, E., and Wallace, D. W. R.: Measurements of organic species in air and seawater  
978 from the tropical Atlantic, *Geophysical Research Letters*, 31, 10.1029/2004gl020012, 2004.

979 Wisthaler, A.: Organic trace gas measurements by PTR-MS during INDOEX 1999, *Journal of Geophysical Research*, 107,  
980 10.1029/2001jd000576, 2002.

981 White, M. L., Russo, R. S., Zhou, Y., Mao, H., Varner, R. K., Ambrose, J., Veres, P., Wingenter, O. W., Haase, K., Stutz, J., Talbot,  
982 R., and Sive, B. C.: Volatile organic compounds in northern New England marine and continental environments during the  
983 ICARTT 2004 campaign, *Journal of Geophysical Research*, 113, 10.1029/2007jd009161, 2008.

984 Wyche, K. P., Monks, P. S., Ellis, A. M., Cordell, R. L., Parker, A. E., Whyte, C., Metzger, A., Dommen, J., Duplissy, J., Prevot,  
985 A. S. H., Baltensperger, U., Rickard, A. R., and Wulfert, F.: Gas phase precursors to anthropogenic secondary organic aerosol:  
986 detailed observations of 1,3,5-trimethylbenzene photooxidation, *Atmos. Chem. Phys.*, 9, 635-665, 10.5194/acp-9-635-2009, 2009.

987 Xiao, Q., Li, M., Liu, H., Fu, M., Deng, F., Lv, Z., Man, H., Jin, X., Liu, S., and He, K.: Characteristics of marine shipping  
988 emissions at berth: profiles for particulate matter and volatile organic compounds, *Atmos. Chem. Phys.*, 18, 9527-9545,  
989 10.5194/acp-18-9527-2018, 2018.

990 Yang, M., Beale, R., Liss, P., Johnson, M., Blomquist, B., and Nightingale, P.: Air–sea fluxes of oxygenated volatile organic  
 991 compounds across the Atlantic Ocean, *Atmospheric Chemistry and Physics*, 14, 7499–7517, 10.5194/acp-14-7499-2014, 2014.

992 Youssef, M. A., Wahid, S. S., Mohamed, M. A., and Askalany, A. A.: Experimental study on Egyptian biomass combustion in  
 993 circulating fluidized bed, *Applied Energy*, 86, 2644–2650, <https://doi.org/10.1016/j.apenergy.2009.04.021>, 2009.

994 Yuan, B., Shao, M., de Gouw, J., Parrish, D. D., Lu, S., Wang, M., Zeng, L., Zhang, Q., Song, Y., Zhang, J., and Hu, M.: Volatile  
 995 organic compounds (VOCs) in urban air: How chemistry affects the interpretation of positive matrix factorization (PMF) analysis,  
 996 *Journal of Geophysical Research: Atmospheres*, 117, n/a–n/a, 10.1029/2012jd018236, 2012.

997 Yuan, B., Warneke, C., Shao, M., and de Gouw, J. A.: Interpretation of volatile organic compound measurements by proton-  
 998 transfer-reaction mass spectrometry over the deepwater horizon oil spill, *International Journal of Mass Spectrometry*, 358, 43–48,  
 999 10.1016/j.ijms.2013.11.006, 2014.

1000 Yuan, B., Koss, A. R., Warneke, C., Coggon, M., Sekimoto, K., and de Gouw, J. A.: Proton-Transfer-Reaction Mass Spectrometry:  
 1001 Applications in Atmospheric Sciences, *Chem Rev*, 117, 13187–13229, 10.1021/acs.chemrev.7b00325, 2017.

1002 Zhao, J., and Zhang, R.: Proton transfer reaction rate constants between hydronium ion (H<sub>3</sub>O<sup>+</sup>) and volatile organic compounds,  
 1003 *Atmospheric Environment*, 38, 2177–2185, 10.1016/j.atmosenv.2004.01.019, 2004.

1004 Zhou, S., Gonzalez, L., Leithead, A., Finewax, Z., Thalman, R., Vlasenko, A., Vagle, S., Miller, L. A., Li, S. M., Burekul, S.,  
 1005 Furutani, H., Uematsu, M., Volkamer, R., and Abbatt, J.: Formation of gas-phase carbonyls from heterogeneous oxidation of  
 1006 polyunsaturated fatty acids at the air–water interface and of the sea surface microlayer, *Atmospheric Chemistry and Physics*, 14,  
 1007 1371–1384, 10.5194/acp-14-1371-2014, 2014.

1008 Zhou, X., and Mopper, K.: Carbonyl compounds in the lower marine troposphere over the Caribbean Sea and Bahamas, *Journal*  
 1009 *of Geophysical Research: Oceans*, 98, 2385–2392, 10.1029/92jc02772, 1993.

1010 Zhou, X., and Mopper, K.: Photochemical production of low-molecular-weight carbonyl compounds in seawater and surface  
 1011 microlayer and their air-sea exchange, *Marine Chemistry*, 56, 201–213, [https://doi.org/10.1016/S0304-4203\(96\)00076-X](https://doi.org/10.1016/S0304-4203(96)00076-X), 1997.